

復旦大學

本科畢業論文



Topological defect lines in 2d CFT

二维共形场论中的拓扑线缺陷

姓 名: 林 易 理 学 号: 20307130021
院 系: 物理学系 专 业: 物 理 学
指导教师: Satoshi Nawata 青年研究员
完成日期: 2024 年 6 月 4 日

Topological defect lines in 2d CFTs

Yili Lin

Abstract

We consider the topological defect lines (TDLs) in two-dimensional conformal field theories. TDLs generalize and encompass the global symmetries and Verlinde lines together with their attached defect operators, forming fusion categories without braiding. We study the crossing relations of TDLs and discuss their relation with the 't Hooft anomaly and orbifolds. We also study the TDLs in rational CFTs, where they can impose constraints on the spin of the defect operators.

Contents

1	Introduction	4
2	Preliminary on conformal field theories	5
2.1	Conformal invariance	5
2.2	Radial quantization and State operator correspondence	6
2.3	Primary field, operator product expansion, and Virasoro algebra . .	7
2.4	Torus partition function	8
2.5	Minimal models	9
2.5.1	Definition and properties	9
2.5.2	Conformal blocks	10
2.6	Rational conformal field theory	10
3	Basis of topological Defect Lines	11
3.1	Definition and properties	11
3.2	Corollaries	16
3.2.1	H-junction crossing relation and Pentagon identity	16
3.2.2	Conditions for Vacuum expectation value $\langle \mathcal{L} \rangle$ and twisted Hilbert space $\mathcal{H}_{\mathcal{L}}$	18
3.2.3	Fusion Coefficient	20
3.3	Isotopy anomaly	20
4	Application of invertible lines	22
4.1	Invertible TDLs and 't Hooft anomaly	22
4.2	Cyclic permutation map and spin selection rule	23
4.2.1	Example: $U(1)$ rotation in free boson on S^1	26
5	Topological defect lines in rational CFTs	27
5.1	The non-invertible TDL \mathcal{N} and the Tambara-Yamagami category .	27
5.2	Verlinde lines	29
5.3	Ising model	30
5.4	Spin selection rule with the non-invertible \mathcal{N}	33
5.4.1	TY(\mathbb{Z}_2) spin selection rule	34
5.4.2	TY(\mathbb{Z}_3) spin selection rule	35
5.5	Brief introduction to TDLs in other models	35
5.5.1	Tricritical Ising model	35
5.5.2	Lee-Yang model	36
5.5.3	Three-state Potts model	36

1 Introduction

Conformal field theories (CFTs) are quantum field theories with the spacetime symmetry enhanced from Lorentz invariance to conformal invariance, which includes scale transformations and special conformal transformations in addition. This enhanced symmetry imbues CFTs with a rich structure and makes them a powerful tool in theoretical physics. In particular, two-dimensional (2d) CFTs defined on an Euclidean 2d spacetime have proven to be especially fruitful. In 2d, the local conformal transformation is infinite-dimensional, which allows for many exact solutions and gives rise to various applications.

2d CFTs are characterized by local point-like operators, including primaries and descendants which originate in Virasoro algebra, together with the operator-state correspondence. CFT operators are subject to the associativity of operator product expansion (OPE) and, in addition, the modular invariance for the 2d torus case. There has been much research on the extended objects called 'defects', such as boundary conditions [1] and line defects/interfaces [2–22], which can be defined by their action on local operators.

A fundamental example is a global symmetry group element $g \in G$, which is a linear transformation of the local operators that preserves the OPEs. The action of g on a local operator can be seen as the contraction of a loop of a topological defect line (TDL) around the local operator. A TDL corresponding to a global symmetry group element is referred to as invertible in this paper, as it is a symmetry action and thus must have an inverse.

In all known instances of global symmetries in CFTs, the invertible TDLs exhibit a strong locality property, meaning they can terminate on defect operators, which obey an extended set of OPEs. In the case of a continuous global symmetry like $U(1)$, Noether's theorem dictates that there must be a conserved spin-one current j_μ , the contour integral of which then defines a family of invertible TDLs labeled by $\theta \in S^1$, where the topological property is derived from the conservation equation. As for discrete global symmetry such as \mathbb{Z}_n , the corresponding invertible TDLs with the above-mentioned properties can be considered as a discrete version of Noether's theorem. It has nontrivial implications on the action of g on local operators that do not obviously follow from the standard axioms on local operators.

Moreover, there are TDLs that do not correspond to any global symmetries, and they are common in 2d CFTs. These general TDLs obey fusion rules that are not group-like. Although invariant under isotopy transformations by definition, a general TDL cannot simply be cut and reconnected. Instead, it must obey non-trivial crossing relations under the splitting/joining operation, which correspond to the Pentagon identity in the mathematical language of the fusion category.

A special class of TDLs, known as the Verlinde lines, exist in rational CFTs (RCFTs) with diagonal modular invariant partition functions. The fusion rules of the Verlinde lines in an RCFT are formally identical to those of the representations

of the chiral vertex algebra. However, the physical interpretation of the fusion of Verlinde lines is entirely different from the OPEs.

We will review the basics and key features of CFT that will be used in this article in Section 2. Then, we will begin the study of TDLs by describing a set of physically motivated defining properties in Section 3. In the context of global symmetry groups, we will discuss 't Hooft anomalies, orbifolds, and discrete torsion related to invertible TDLs in Section 4. In Section 5, we discuss TDLs in rational CFTs that are generally not invertible. Particularly, in Section 5.1, we introduce a typical type of non-invertible TDL that plays a role in many CFTs including the Ising model. In Section 5.2 we introduce the Verlinde lines, and describe the explicit crossing relations of Verlinde lines in the critical Ising model in Section 5.3. We also briefly introduce the Verlinde lines in other models in Section 5.5

This paper aims to explore the possible types of TDLs realized in unitary, compact 2d CFTs and their constraints on the dynamics of CFTs after obtaining the fusion and crossing relations, one of which is the restriction on the spin of defect operators in Hilbert space twisted by TDLs. Typically, only specific fractional spins are allowed for the defect operators. This is discussed in Section 5.4. Our main reference is [23]. For the defining properties of TDLs, we also refer to [24].

2 Preliminary on conformal field theories

In this section, we introduce the basics and key features of CFT that will be used in the article. We mostly refer to [25].

2.1 Conformal invariance

The mathematical definition of conformal transformation is a smooth map between two manifolds equipped with metric $f : (M, g) \rightarrow (M', g')$ that satisfies

$$f^*g' = \alpha g \tag{2.1}$$

where f^* is the pull-back map induced by f , and α should be a scalar function on M . In physical language, $(M, g) = (M', g')$ is the spacetime manifold and the definition can be expressed in coordinates as

$$g'_{\rho\sigma}(x') \frac{\partial x'^\rho}{\partial x^\mu} \frac{\partial x'^\sigma}{\partial x^\nu} = \alpha(x) g_{\mu\nu}(x) \tag{2.2}$$

We can see that the special case of $\alpha = 1$ and $g = \pm(+---)$ is just the Lorentz invariance.

From this definition, we can derive that infinitesimal conformal transformation $x \rightarrow x + \epsilon$ should satisfy

$$\partial_\mu \epsilon_\nu + \partial_\nu \epsilon_\mu = \frac{2}{d} \partial_\rho \epsilon^\rho g_{\mu\nu} \tag{2.3}$$

where $d = \dim_{\mathbb{R}} M$ is the spacetime dimension. This equation will give us the generators of conformal transformation, where we will see the special of $d = 2$.

For a general spacetime dimension $d \geq 3$, the generators are the translation $-i\partial_\mu$, rotation $i(x_\mu\partial_\nu - x_\nu\partial_\mu)$, dilation $-ix^\mu\partial_\mu$ and the special conformal transformation (SCT) $-i(2x_\mu x^\nu\partial_\nu - x^\nu x_\nu\partial_\mu)$. The former two generators are familiar ones in Lorentz transformation, while the dilation corresponds to a finite scaling $x \rightarrow a \cdot x$ and the SCT actually corresponds to a combination of inversion-translation-inversion. Because the inversion $x \rightarrow \frac{x}{x \cdot x}$ doesn't have an infinitesimal version, the SCT shows up.

For $d = 2$ with the Euclidean metric $g_{\mu\nu} = \text{diag}(1, 1)$, the condition (2.3) is equivalent to the Cauchy-Riemann condition $\partial_1\epsilon_2 = -\partial_2\epsilon_1, \partial_1\epsilon_1 = \partial_2\epsilon_2$. Then we know that all the holomorphic map $f(x, y) = f(x + iy) = f(z) \in \mathbb{C} \cup \infty$ are conformal transformations, which is a much looser condition than the $d > 3$ case where there are only four generators, as generators for a holomorphic map are infinitely many.

Yet we can notice that a general $f(z)$ may have high order singularities at certain points on $\mathbb{C} \cup \infty$ and is thus non-invertible. If we only consider the invertible ones on $\mathbb{C} \cup \infty$, i.e. the global transformations, we will again obtain the translation, rotation, dilation, and SCT. Combining them we have the form $f(z) = \frac{az+b}{cz+d}$, $ad - bc = 1$, which is called Möbius transformation and forms a group $SL(2, \mathbb{C})/\mathbb{Z}_2 = PGL(2, \mathbb{C})$.

One typical result of conformal invariance is that any four points (x_1, x_2, x_3, x_4) are equivalent to $(0, 1, x = \frac{(x_1-x_2)(x_3-x_4)}{(x_1-x_3)(x_2-x_4)}, \infty)$. This can be shown as follows: first use translation and inversion to move x_4 to ∞ , then translate x_1 to 0 and finally dilate x_2 to 1. This process works in both $d = 2$ and $d \geq 3$.

2.2 Radial quantization and State operator correspondence

Let $z = t+ix$ describe a point on a cylinder by $x \sim x+2\pi$ being the cyclic direction. Considering the map $w \rightarrow z = e^w$, we can see that the t direction becomes the radial direction while the cyclic x direction becomes the angular direction. Then the translation in t corresponds to the dilation of z while the translation in x corresponds to the rotation of ϕ . The time order in ordinary QFT quantization also becomes radius order. This setting is called the radial quantization.

With radial quantization, an initial state at past infinity on the cylinder corresponds to an operator inserted at the origin of the plane

$$|\phi_{in}\rangle = \phi(0, 0) |0\rangle \quad (2.4)$$

which is the state-operator correspondence.

Also, we know that the Hamiltonian H is the generator of temporal translation, which becomes radial dilation under radial quantization, while the momentum P is the generator of spatial translation, which becomes angular translation. In polar

coordinates $z = re^{i\phi}$, we have $r\partial_r = z\partial_z + \bar{z}\partial_{\bar{z}}$, $\partial_\phi = i(z\partial_z - \bar{z}\partial_{\bar{z}})$. Thus H and P are just

$$H = L_0 + \bar{L}_0 \quad P = i(L_0 - \bar{L}_0) \quad (2.5)$$

where L_0, \bar{L}_0 are the zero modes in the expansion of energy-momentum tensor $-2\pi T_{zz}(z) = T(z) = \sum_{n \in \mathbb{Z}} \frac{L_n}{z^{n+2}} \Leftrightarrow L_n = \frac{1}{2\pi i} \oint dz z^{n+1} T(z)$ together with the anti-holomorphic part.

Note that under the cylinder-to-plane map, L_0 also transforms as

$$L_{0,cyl} = L_{0,pl} - \frac{c}{24} \quad (2.6)$$

which results in a $\frac{c}{12}$ in H_{cyl} .

2.3 Primary field, operator product expansion, and Virasoro algebra

When applying the conformal spacetime to the field theory, many concepts such as the Noether theorem, energy-momentum tensor, correlation function, and Ward-Takahashi identity are analogous, while a new concept lies in the transformation of fields under the spacetime transformation.

Consider the generators $z\partial_z, \bar{z}\partial_{\bar{z}}$ accounting for dilation and rotation, a physical state should be an eigenstate of them, where the eigenvalues (h, \bar{h}) are called conformal dimensions, describing the transformation of the field ϕ as $\phi \rightarrow \lambda^{-h} \bar{\lambda}^{-\bar{h}} \phi$ under $z \rightarrow \lambda z$. We define the primary field to satisfy $\phi \rightarrow (\frac{dz'}{dz})^{-h} (\frac{d\bar{z}'}{d\bar{z}})^{-\bar{h}} \phi$ under any holomorphic $z \rightarrow z'$. If this is satisfied under only global $z \rightarrow z'$, we call ϕ a quasi-primary field.

With this definition, the Ward-Takahashi identity of primary fields tells us that inserting energy-momentum tensor $T(z) = -2\pi T_{zz}(z)$ in primary correlators of $\phi(z_i)$ produces

$$\langle T(z)\phi(z_i) \rangle = \frac{1}{z - z_i} \partial_{z_i} \phi_i + \frac{h_i}{(z - z_i)^2} \phi_i + \text{terms regular at } z = z_i \quad (2.7)$$

Expressions like this are called the operator product expansion (OPE), and $\langle \rangle$ is often omitted. A general result of OPE is that

$$T(z)T(w) \sim \frac{c/2}{(z-w)^4} + \frac{2}{(z-w)^2} T(w) + \frac{1}{z-w} \partial_w T(w) \quad (2.8)$$

where c is called the central charge. Furthermore, remember the expansion of $T(z)$: $L_n = \frac{1}{2\pi i} \oint dz z^{n+1} T(z)$, TT OPE (2.8) tells us that

$$[L_n, L_m] = (n - m)L_{n+m} + \frac{c}{12}n(n^2 - 1)\delta_{n+m,0} \quad (2.9)$$

which is called the Virasoro algebra $Vir \ni L_n$. There is a similar one $\bar{Vir} \ni \bar{L}_n$ for the antiholomorphic part.

With the above results, we can find that primary states $\phi(0,0)|0\rangle$ are just eigenstates of L_0, \bar{L}_0 with eigenvalues being the conformal dimension h, \bar{h} of ϕ . We can just rewrite $\phi(0,0)|0\rangle = |h, \bar{h}\rangle$. The Virasoro algebra further tells us that $L_{-i}\bar{L}_{-j}L\dots|h, \bar{h}\rangle$ ($i, j, \dots > 0$) have eigenvalues $h + i + \dots, \bar{h} + j + \dots$ for L_0, \bar{L}_0 . These states are called descendants states of $|h, \bar{h}\rangle$, and $h + i + \dots, \bar{h} + j + \dots$ are called their levels. $|h, \bar{h}\rangle$ and its descendants form a representation of Virasoro algebra, called the Verma module $V(c, h) \otimes \bar{V}(c, \bar{h})$. The conformal dimension (h, \bar{h}) of the primary ϕ this representation is based on is called the highest weight of the representation. In a Verma module, $L_{n>0}$ can be interpreted as annihilation operators while $L_{n<0}$ as creation operators.

From the OPE of primaries, we can also derive that the OPE of descendants can be obtained by acting some specific operators on the OPE of primaries. That is to say, the OPEs of primaries are enough to determine the OPE of arbitrary operators. We call the set of a primary ϕ and its descendants a conformal family $[\phi]$.

Inside a Verma module $V(c, h)$ of $|h\rangle$, there may exist states $|\chi\rangle \neq |h\rangle$ annihilated by all the $L_{n<0}$. This makes $|\chi\rangle$ orthogonal to all the other states i.e., $\langle\chi| L_{n<0}|h\rangle = 0$. $|\chi\rangle$ is called a null state. Descendants generated by acting on $|\chi\rangle$ are all null states, therefore, the existence of null states means that this Verma module $V(c, h)$ can be reduced by taking quotient over the null states.

2.4 Torus partition function

In CFT, the spacetime $\mathbb{C} \cup \infty$ is often set to have a torus structure, which means identifying $z \sim z + m\sigma_1 + n\sigma_2$ ($m, n \in \mathbb{Z}$). Define $\tau = \frac{\sigma_2}{\sigma_1} = \tau_1 + i\tau_2$ to describe the torus, we can find that many τ 's actually describe the same torus. Precisely,

$$\tau' = \frac{a\tau + b}{c\tau + d} \quad \text{where } \begin{pmatrix} a & b \\ c & d \end{pmatrix} \in SL(2, \mathbb{Z})/\mathbb{Z}_2 \quad (2.10)$$

doesn't change the torus. The group $SL(2, \mathbb{Z})/\mathbb{Z}_2$ is called the modular group or the mapping class group of the torus and can be generated by two elements: S: $\tau \rightarrow -\frac{1}{\tau}$ and T: $\tau \rightarrow \tau + 1$.

The partition function of CFT on torus contains τ , i.e., $Z = Z(\tau)$. As mentioned above, the torus remains the same under transformations generated by S and T, so should Z . This modular invariance yields critical conditions for CFTs.

The partition function should take the form $Z = \text{Tr}_{\mathcal{H}}(e^{-2\pi\tau_2 H} e^{2\pi\tau_1 P})$, where \mathcal{H} is the Hilbert space and H, P are the Hamiltonian and momentum. Apply (2.5),(2.6) and let $q = e^{2\pi i\tau}$, we have

$$Z(\tau) = \text{Tr}_{\mathcal{H}}\left(q^{L_{0,pl}-\frac{c}{24}} \bar{q}^{\bar{L}_{0,pl}-\frac{c}{24}}\right) \quad (2.11)$$

2.5 Minimal models

2.5.1 Definition and properties

Minimal models are models with finitely many primary fields, consequently finitely many highest weights of representations. In the sections before we have mentioned the null states in a Verma module, and it turns out that there exists an expression $h_{r,s}(c)$ with parameters r, s which indicates that the Verma module of $|h_{r,s}(c)\rangle$ has a null state at level rs . Furthermore, the existence of null states imposes conditions on the correlators, which produce the operator algebra like

$$\phi_{r_1,s_1} \times \phi_{r_2,s_2} = \sum_{k,l(r,s)} [\phi_{k,l}] \quad (2.12)$$

which means OPE of two primaries with dimension $h_{r_1,s_1}(c)$ and $h_{r_2,s_2}(c)$ contains operators in family of $h_{k,l}$ dimension primaries, where range of k, l is determined by r, s .

Such an expression means that if the number of $h_{r,s}(c)$ is to be finite, we demand a periodicity $h_{r,s}(c) = h_{r+p,s+p'}$. This condition gives a minimal model $\mathcal{M}_{p,p'}$, and it turns out that

$$c = 1 - 6 \frac{(p-p')^2}{pp'} \quad (2.13)$$

$$h_{r,s} = \frac{(p'r-ps)^2 - (p-p')^2}{4pp'} \quad (2.14)$$

On the other hand, the unitarity of the states in the Verma module demands that $|p' - p| = 1$. Thus unitary minimal models $\mathcal{M}_{p,p+1}$ have

$$c = 1 - 6 \frac{1}{p(p+1)} \quad (2.15)$$

$$h_{r,s} = \frac{((p+1)r-ps)^2 - 1}{4p(p+1)} \quad (2.16)$$

Another important feature of the minimal models is that their torus partition functions take the form

$$Z(\tau, \bar{\tau}) = \sum_{h,\bar{h}} n_{h,\bar{h}} \chi_h(\tau) \bar{\chi}_{\bar{h}}(\bar{\tau}) \quad (2.17)$$

where $n_{h,\bar{h}}$ means the number of primaries of dimension (h, \bar{h}) , and

$$\chi_h(\tau) = \text{Tr}_{L(c,h)} \left(q^{L_0 - \frac{c}{24}} \right) \quad (2.18)$$

where $L(c, h)$ denotes the irreducible representation of Virasoro algebra derived from the Verma module $V(c, h)$.

2.5.2 Conformal blocks

Because of the finiteness of primaries, the coefficients in a minimal model can be all determined in principle. One method is to use the conformal blocks, which are defined as

$$\mathcal{F}(1, 2, 3, 4; p|x) = x^{h_p - h_3 - h_4} \sum_{\{k_i\}} \beta_{34}^{p(\{k_i\})} x^{\sum k_i} \frac{\langle h_1 | \phi_2(1) L_{-\{k_i\}} | h_p \rangle}{\langle h_1 | \phi_2(1) | h_p \rangle} \quad (2.19)$$

It originates in the four-point function

$$\begin{aligned} & \langle \phi_1(\infty, \infty), \phi_2(1, 1), \phi_3(x, x), \phi_4(0, 0) \rangle \\ &= \sum_p C_{12p} C_{34p} \mathcal{F}(1, 2, 3, 4; p|x) \bar{\mathcal{F}}(1, 2, 3, 4; p|\bar{x}) \end{aligned} \quad (2.20)$$

where p denotes the primaries and C is the three-point coefficient. The coordinates $(\infty, 1, x, 0)$ can be transformed to arbitrary four points, as we have seen before. The above equation comes after first fusing ϕ_3, ϕ_4 to $[\phi_p]$, then considering the three-point function of $[\phi_p], \phi_1, \phi_2$. If the conformal blocks are known, the equivalence between the 12-34 channel of coordinates $(\infty, 1, x, 0)$ and the 23-14 channel of coordinates $(\infty, 1, x, 0)$ can give us

$$\begin{aligned} & \sum_p C_{12p} C_{34p} \mathcal{F}(1, 2, 3, 4; p|x) \bar{\mathcal{F}}(1, 2, 3, 4; p|\bar{x}) \\ &= \sum_q C_{14q} C_{23q} \mathcal{F}(1, 4, 2, 3; q|1-x) \bar{\mathcal{F}}(1, 2, 3, 4; q|1-\bar{x}) \end{aligned} \quad (2.21)$$

which is called the crossing symmetry. For minimal models, such equations suffice to solve the three-point coefficients C 's. This strategy is called the conformal bootstrap.

2.6 Rational conformal field theory

Rational conformal field theories (RCFT) is a greater class of CFT including the minimal models. In RCFT, the algebra can be extended beyond the Virasoro algebra $Vir \otimes \overline{Vir}$ to some chiral algebra $A \otimes \overline{A}$, which contains the Virasoro as a subalgebra.

An RCFT is defined to be unitary with a unique vacuum, and have finitely many primary fields of the chiral algebra $A \otimes \overline{A}$. Then, the Hilbert space should be spanned by $\mathcal{H} = \bigoplus_{i,j} n_{i,j} V_i \otimes \overline{V}_j$, where V_i is the irreducible representation arises from primary ϕ_i . The partition function of an RCFT takes a form similar to (2.17), which will be discussed in Section 5.2

The conformal dimensions of primary fields as well as the central charge of RCFT are rational numbers. The crossing symmetries in RCFT are also solvable in principle, and one can evaluate a correlation function on an arbitrary Riemann surface.

3 Basis of topological Defect Lines

3.1 Definition and properties

TDLs are depicted by oriented lines in 2d CFT. They act on local states when passing through one, create twisted Hilbert space at endpoints, and fit the fusion rule:

$$\mathcal{L}_i \mathcal{L}_j = \sum_k N_{ij}^k \mathcal{L}_k \quad (3.1)$$

with an identity element I . There exists an orientation-reversed TDL $\bar{\mathcal{L}}$ for every TDL \mathcal{L} . A TDL \mathcal{L} is called invertible if $\mathcal{L}\bar{\mathcal{L}} = I$, while the general case is

$$\mathcal{L}\bar{\mathcal{L}} = I + \sum_k N^k \mathcal{L}_k \quad (3.2)$$

The motivation for defining TDLs is that they can form a representation of the global symmetry group G , by corresponding each element $g \in G$ to a certain TDL \mathcal{L}_g , together with the algebra of the symmetry group $\mathcal{L}_{g_1} \mathcal{L}_{g_2} = \mathcal{L}_{g_1 g_2}$, which is compatible with the fusion rule (3.1). The definition and properties of TDLs also include the following.

1. **Isotopy invariance** Correlation functions are invariant under ambient isotopic deformation of the graph involving TDLs embedded in the flat spacetime. This is a formal way of saying that TDLs are topological objects. Isotopy invariance leads to the commutation of TDLs with the energy-momentum tensor.
2. **Action on local operator** A TDL \mathcal{L} induces a map $\hat{\mathcal{L}} : \mathcal{H} \rightarrow \mathcal{H}$ by wrapping a loop around the spatial circle, mapping a local operator ϕ to another $\hat{\mathcal{L}} \cdot \phi$ while conserving the conformal weight (h, \bar{h}) , as shown in Fig.1. In special cases of invertible TDLs that correspond to global symmetries, the map is just the action of the symmetry group element $\hat{g} : \mathcal{H} \rightarrow \mathcal{H}$.

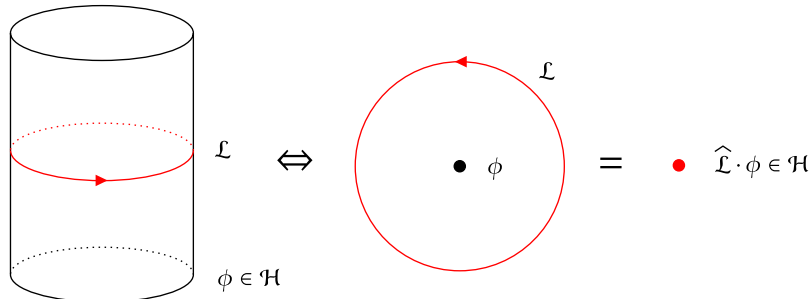


Figure 1: A TDL \mathcal{L} in the spatial direction acting on a local operator, in cylindrical and planar diagram

We can also define the vacuum expectation value $\langle \mathcal{L} \rangle = \langle 0 | \mathcal{L} | 0 \rangle$ on the cylinder, which implies that $\widehat{\mathcal{L}} | 0 \rangle = \langle \mathcal{L} | 0 \rangle$ because \mathcal{L} must preserve vacuum $| 0 \rangle$. Then the commutation between a local operator ϕ and a TDL \mathcal{L} becomes $\widehat{\mathcal{L}} | \phi \rangle = \langle \mathcal{L} | \phi \rangle$.

3. Twisted Hilbert space By attaching an endpoint to a TDL \mathcal{L} instead of wrapping a loop, one gets a twisted Hilbert space $\mathcal{H}_{\mathcal{L}}$ at the endpoint, from which \mathcal{L} is outgoing in our convention. The operators in this twisted Hilbert space are called defect operators. This configuration can be interpreted as a time-oriented TDL along the cylinder with a defect operator on the past infinity circle, as shown in Fig.2.

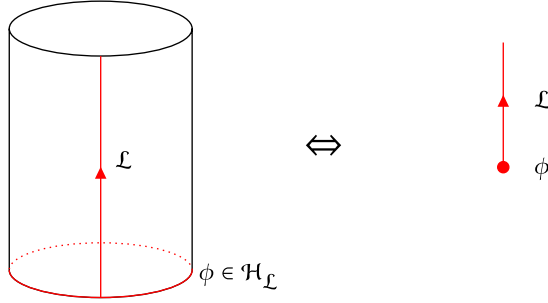


Figure 2: A TDL \mathcal{L} in the temporal direction with a defect operator attached, in cylindrical and planar diagram

Similarly, one can join multiple TDLS at one point, which is called a junction, with a twisted Hilbert space $\mathcal{H}_{\mathcal{L}_1, \mathcal{L}_2, \dots}$. If a junction is to be topological, the operator at the point must have conformal weight $(0, 0)$, which is called a junction vector. A typical junction with three TDLS is shown in Fig.3. The subspace $V_{\mathcal{L}_1, \mathcal{L}_2, \dots}$ of $(0, 0)$ states in $\mathcal{H}_{\mathcal{L}_1, \mathcal{L}_2, \dots}$ is called a junction vector space. A cyclic permutation (such as changing $V_{\mathcal{L}_1, \mathcal{L}_2, \dots}$ to $V_{\mathcal{L}_2, \mathcal{L}_3, \dots}$) could have a non-trivial effect on the junction.

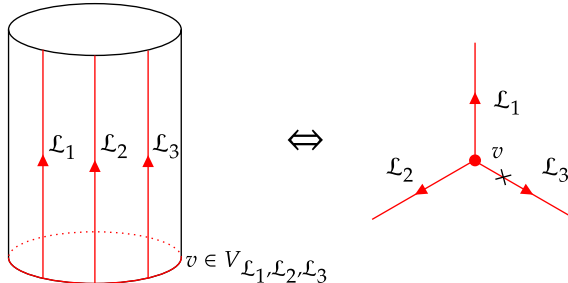


Figure 3: Three TDLS $\mathcal{L}_1, \mathcal{L}_2, \mathcal{L}_3$ joining in one topological junction v , in cylindrical and planar diagram. The "x" marks the last TDL, clarifying the permutation.

As shown in Fig.4, one simple diagram that involves both the local operator and the junction is a "lasso", where a TDL \mathcal{L} encircles a local operator ϕ and joins another TDL \mathcal{L}' with a junction vector $v \in V_{\mathcal{L}, \bar{\mathcal{L}}, \mathcal{L}'}$. By contracting \mathcal{L} , one obtains a defect operator $\widehat{\mathcal{L}}^v \cdot \phi \in \mathcal{H}_{\mathcal{L}'}$ attached to the TDL \mathcal{L}' .

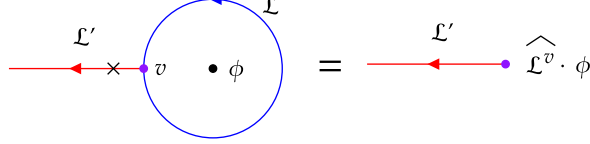


Figure 4: "Lassoing" the local operator ϕ with \mathcal{L} attached to \mathcal{L}' produces $\widehat{\mathcal{L}^v} \cdot \phi \in \mathcal{H}_{\mathcal{L}'}$

One property of the junction vector space is that $V_{\mathcal{L} \neq I}$ must be empty, because otherwise any \mathcal{L} loop could be unwrapped from a point and all local operators would commute with \mathcal{L} , which would require \mathcal{L} to be I .

4. Partial Fusion As shown in Fig.5, two TDLs $\mathcal{L}_1, \mathcal{L}_2$ can also be partially fused to $\mathcal{L}_1 \mathcal{L}_2$ with uniquely determined junction vectors $\sum_i v_i \otimes v'_i \in V_{\mathcal{L}_1, \mathcal{L}_2, \overline{\mathcal{L}_1 \mathcal{L}_2}} \otimes V_{\mathcal{L}_2, \mathcal{L}_1, \mathcal{L}_1 \mathcal{L}_2}$.

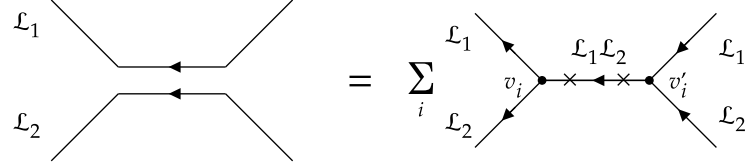


Figure 5: Partial fusion of $\mathcal{L}_1, \mathcal{L}_2$

Combining this property with lassoing, one can move a TDL \mathcal{L} past a local operator ϕ , leaving behind another TDL $\widehat{\mathcal{L}}$ and a defect operator $\widehat{\mathcal{L}^v} \cdot \phi$, as shown in Fig.6. When \mathcal{L} and ϕ commute, this also leads to $\widehat{\mathcal{L}^v} \cdot \phi = 0$.

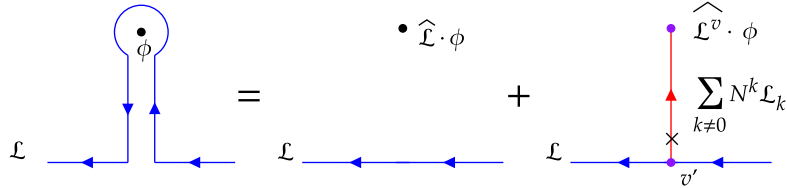


Figure 6: Moving \mathcal{L} past ϕ , applying partial fusion, "lasso" and (3.2). When \mathcal{L} and ϕ commute, the last term vanishes, and $\widehat{\mathcal{L}} \cdot \phi = \phi$

5. Correlation functional TDLs generalize correlation functions by replacing local operators with defect ones, together with TDLs starting at defect operators and joining one another at junctions. Such a graph with TDL configuration and a given set of defect and local operators introduce a multi-linear complex-valued function on the tensor product of junction vector spaces, which is called a correlation functional.

Correlation functionals have isotopy invariance in the flat spacetime, as a defining property of TDLs. When extending this property to curved surfaces, however,

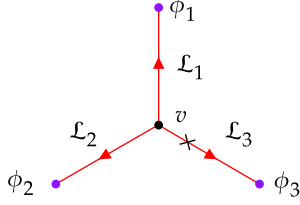


Figure 7: An example of correlation functional, constructed by three TDLs. This introduces a map: $V_{\mathcal{L}_1, \mathcal{L}_2, \mathcal{L}_3} \rightarrow \mathbb{C}$

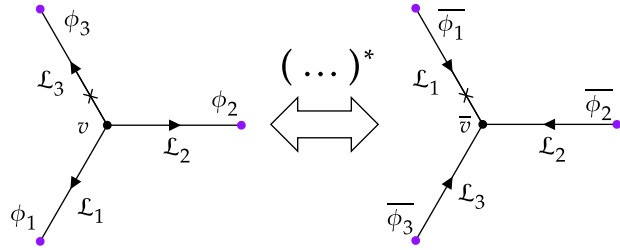


Figure 8: Conjugation map in a correlation function. The TDLs are reversed and the operators are replaced with their operator conjugation, both of whose locations are changed to the complex conjugation.

the correlation functional may acquire a phase proportional to the integral of the curvature over the region swept by the deformation of TDLs. Such a property is called isotopy anomaly, and will be discussed in Section 3.3.

6. Conjugation The conjugation of a defect operator $\phi \in \mathcal{H}_{\mathcal{L}_1, \mathcal{L}_2, \dots, \mathcal{L}_k}$ should lie in $\mathcal{H}_{\mathcal{L}_k, \mathcal{L}_{k-1}, \dots, \mathcal{L}_1}$. Define the conjugation $\phi^* \in \mathcal{H}_{\mathcal{L}_k, \mathcal{L}_{k-1}, \dots, \mathcal{L}_1}$ of ϕ so that the two-point function $h(\phi_1, \phi^*)$ of a pair of defect operators $\phi_1 \in \mathcal{H}_{\mathcal{L}_1, \mathcal{L}_2, \dots, \mathcal{L}_k}$ and ϕ^* equals the inner product of ϕ_1 and ϕ , i.e.,

$$\phi^* : h(\phi_1, \phi^*) = \langle \phi_1, \phi \rangle \quad (3.3)$$

Acting the conjugation map on all defect operators in a correlation function together with a complex conjugation on their locations $z_i \rightarrow \bar{z}_i$ is equivalent to the complex conjugation of the original correlation function. One result of this property is that the junction vector in the trivial 3-way junction $v \in V_{\mathcal{L}, \bar{\mathcal{L}}, I}$ should have $\langle v, v \rangle = \langle \mathcal{L} \rangle \Rightarrow |v| = \sqrt{\langle v, v \rangle} = \sqrt{\langle \mathcal{L} \rangle}$. Note that for $\langle \mathcal{L} \rangle \neq 1$, the trivial junction vector is not normalized, which should be taken into account in the fusion process.

7. Locality Roughly speaking, locality means a TDL cannot see the whole graph, so that one can find a replacement of a certain part of the graph that produces a different but equivalent TDL graph. Specifically, one can cut the TDL graph along a circle that intersects the TDLs transversely and put on the circle a complete orthonormal basis of Hilbert space associated with that circle. The states on the circle can be constructed by taking a disc with (defect) operators inserted,

which could be further glued back to the graph with a circle boundary. For defect operators inside the circle, this process is equivalent to considering their OPEs. For junctions, the process introduces a multi-linear map from the tensor product of the original junction vector space to the new junction vector space.

As a typical example, when applying this cut-and-glue process to an H-junction like in Fig.9, it introduces a map $H_{\mathcal{L}_2, \mathcal{L}_3}^{\mathcal{L}_1, \mathcal{L}_4}(\mathcal{L}_5) : V_{\mathcal{L}_1, \mathcal{L}_2, \mathcal{L}_5} \otimes V_{\mathcal{L}_3, \mathcal{L}_4, \mathcal{L}_5} \rightarrow V_{\mathcal{L}_1, \mathcal{L}_2, \mathcal{L}_3, \mathcal{L}_4}$

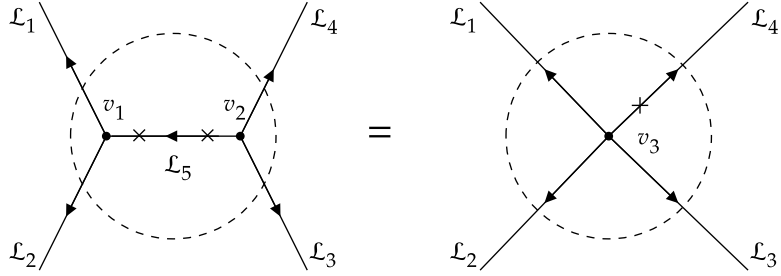


Figure 9: $H_{\mathcal{L}_2, \mathcal{L}_3}^{\mathcal{L}_1, \mathcal{L}_4}(\mathcal{L}_5)$ maps $v_1 \otimes v_2$ to v_3

8. Modular covariance The torus partition function in 2d CFT is always modular invariant due to the torus geometry. The correlation functions of local operators must transform covariantly under the modular group, and so do the correlation functionals with TDLs. Consider a graph with one TDL \mathcal{L}_1 in the time direction and another TDL \mathcal{L}_2 in the spatial direction. The torus partition function is

$$Z_{\mathcal{L}_1}^{\mathcal{L}_2}(\tau) = \text{Tr}_{\mathcal{H}_{\mathcal{L}_1}} \left(\widehat{\mathcal{L}_2} q^{L_0 - \frac{c}{24}} \bar{q}^{\bar{L}_0 - \frac{c}{24}} \right) \quad (3.4)$$

Under the T transformation, the cylinder is twisted around the space circle by one period, so the graph becomes \mathcal{L}_1 in the time direction and $\mathcal{L}_2 \mathcal{L}_1$ in the spatial direction. The torus partition function now becomes

$$Z_{\mathcal{L}_1}^{\mathcal{L}_2 \mathcal{L}_1}(\tilde{\tau}) = \text{Tr}_{\mathcal{H}_{\mathcal{L}_1}} \left(\widehat{\mathcal{L}_2 \mathcal{L}_1} \tilde{q}^{L_0 - \frac{c}{24}} \bar{\tilde{q}}^{\bar{L}_0 - \frac{c}{24}} \right) \quad (3.5)$$

and the modular invariance reads

$$Z_{\mathcal{L}_1}^{\mathcal{L}_2 \mathcal{L}_1}(\tau + 1) = Z_{\mathcal{L}_1}^{\mathcal{L}_2}(\tau) \quad (3.6)$$

Under S transformation, the diagram is rotated 90 degrees, swapping the time direction and space direction. This results in

$$Z_{\mathcal{L}_2^{-1}}^{\mathcal{L}_1}(\tilde{\tau}) = \text{Tr}_{\mathcal{H}_{\mathcal{L}_2^{-1}}} \left(\widehat{\mathcal{L}_1} \tilde{q}^{L_0 - \frac{c}{24}} \bar{\tilde{q}}^{\bar{L}_0 - \frac{c}{24}} \right) \quad (3.7)$$

and

$$Z_{\mathcal{L}_2^{-1}}^{\mathcal{L}_1} \left(-\frac{1}{\tau} \right) = Z_{\mathcal{L}_1}^{\mathcal{L}_2}(\tau) \quad (3.8)$$

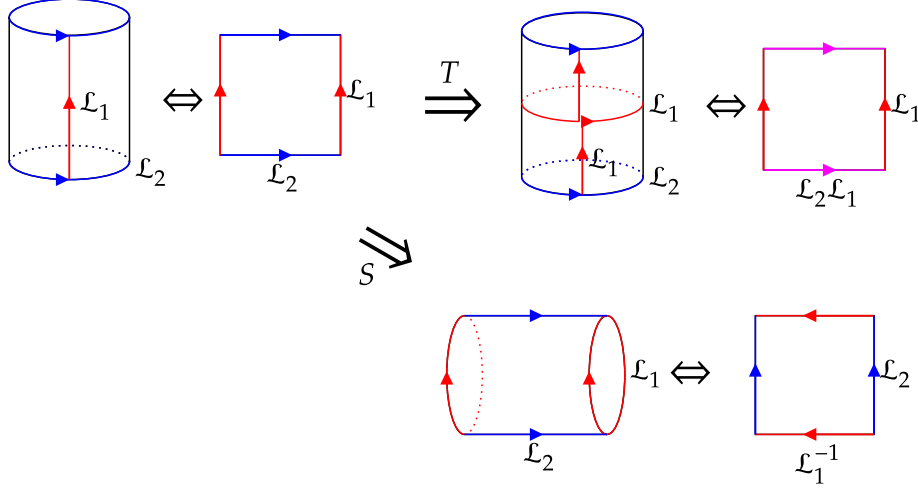


Figure 10: Modular covariance of temporal TDL \mathcal{L}_1 and spatial TDL \mathcal{L}_2 under T and S transformation on torus.

3.2 Corollaries

3.2.1 H-junction crossing relation and Pentagon identity

We have seen from the locality that an H-junction introduces a map $H_{\mathcal{L}_2, \mathcal{L}_3}^{\mathcal{L}_1, \mathcal{L}_4}(\mathcal{L}_5) : V_{\mathcal{L}_1, \mathcal{L}_2, \overline{\mathcal{L}_5}} \otimes V_{\mathcal{L}_3, \mathcal{L}_4, \mathcal{L}_5} \rightarrow V_{\mathcal{L}_1, \mathcal{L}_2, \mathcal{L}_3, \mathcal{L}_4}$. Naturally, we can permute the TDLs so that the map becomes $H_{\mathcal{L}_3, \mathcal{L}_1}^{\mathcal{L}_2, \mathcal{L}_4}(\mathcal{L}_5) : V_{\mathcal{L}_2, \mathcal{L}_3, \overline{\mathcal{L}_5}} \otimes V_{\mathcal{L}_4, \mathcal{L}_1, \mathcal{L}_5} \rightarrow V_{\mathcal{L}_2, \mathcal{L}_3, \mathcal{L}_4, \mathcal{L}_1}$. Since $V_{\mathcal{L}_1, \mathcal{L}_2, \mathcal{L}_3, \mathcal{L}_4}$ and $V_{\mathcal{L}_2, \mathcal{L}_3, \mathcal{L}_4, \mathcal{L}_1}$ are related by a cyclic permutation $C_{\mathcal{L}_1, \mathcal{L}_2, \mathcal{L}_3, \mathcal{L}_4} : V_{\mathcal{L}_1, \mathcal{L}_2, \mathcal{L}_3, \mathcal{L}_4} \rightarrow V_{\mathcal{L}_2, \mathcal{L}_3, \mathcal{L}_4, \mathcal{L}_1}$, we can try to construct a map between $V_{\mathcal{L}_1, \mathcal{L}_2, \overline{\mathcal{L}_5}} \otimes V_{\mathcal{L}_3, \mathcal{L}_4, \mathcal{L}_5}$ and $V_{\mathcal{L}_2, \mathcal{L}_3, \overline{\mathcal{L}_6}} \otimes V_{\mathcal{L}_4, \mathcal{L}_1, \mathcal{L}_6}$. The construction involves the inverse map of $H_{\mathcal{L}_2, \mathcal{L}_3}^{\mathcal{L}_1, \mathcal{L}_4}(\mathcal{L}_5)$, which can be constructed by applying partial fusion and locality as in Fig.11.

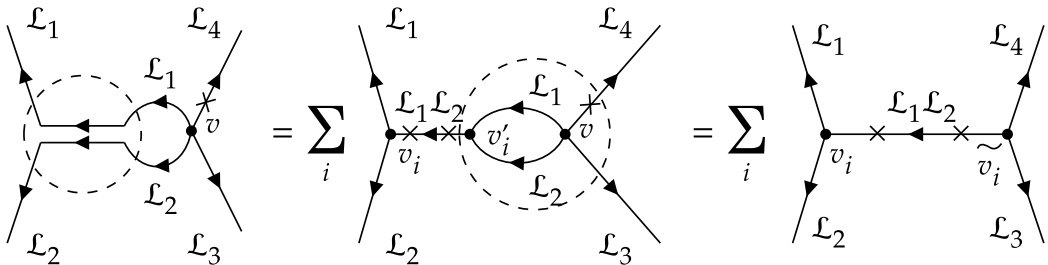


Figure 11: Construction of inverse map $\overline{H}_{\mathcal{L}_2, \mathcal{L}_3}^{\mathcal{L}_1, \mathcal{L}_4}(\mathcal{L}_6)$. Starting with a four-leg junction v , first take the partial fusion of $\mathcal{L}_1, \mathcal{L}_2$, obtaining $\sum_i v_i \otimes v'_i \in V_{\mathcal{L}_1, \mathcal{L}_2, \overline{\mathcal{L}_1 \mathcal{L}_2}} \otimes V_{\mathcal{L}_2, \mathcal{L}_1, \mathcal{L}_1 \mathcal{L}_2}$. Next, apply the cut-and-glue process to the $\mathcal{L}_3, \mathcal{L}_4, \mathcal{L}_1 \mathcal{L}_2$ patch, obtaining a map: $v'_i \otimes v \in V_{\mathcal{L}_2, \mathcal{L}_1, \mathcal{L}_1 \mathcal{L}_2} \otimes V_{\mathcal{L}_1, \mathcal{L}_2, \mathcal{L}_3, \mathcal{L}_4} \rightarrow \tilde{v}'_i \in V_{\mathcal{L}_3, \mathcal{L}_4, \mathcal{L}_1 \mathcal{L}_2}$. Together, we complete the map $\overline{H}_{\mathcal{L}_2, \mathcal{L}_3}^{\mathcal{L}_1, \mathcal{L}_4} : v \in V_{\mathcal{L}_1, \mathcal{L}_2, \mathcal{L}_3, \mathcal{L}_4} \rightarrow \sum_i v_i \otimes \tilde{v}'_i \in V_{\mathcal{L}_1, \mathcal{L}_2, \overline{\mathcal{L}_1 \mathcal{L}_2}} \otimes V_{\mathcal{L}_3, \mathcal{L}_4, \mathcal{L}_1 \mathcal{L}_2}$. Then $\overline{H}_{\mathcal{L}_2, \mathcal{L}_3}^{\mathcal{L}_1, \mathcal{L}_4}(\mathcal{L}_6)$ can be obtained simply by projecting $V_{\mathcal{L}_1, \mathcal{L}_2, \overline{\mathcal{L}_1 \mathcal{L}_2}} \otimes V_{\mathcal{L}_3, \mathcal{L}_4, \mathcal{L}_1 \mathcal{L}_2}$ to $V_{\mathcal{L}_1, \mathcal{L}_2, \overline{\mathcal{L}_6}} \otimes V_{\mathcal{L}_3, \mathcal{L}_4, \mathcal{L}_6}$.

With the inverse map $\overline{H}_{\mathcal{L}_2, \mathcal{L}_3}^{\mathcal{L}_1, \mathcal{L}_4}(\mathcal{L}_6)$, we can define

$$K_{\mathcal{L}_2, \mathcal{L}_3}^{\mathcal{L}_1, \mathcal{L}_4}(\mathcal{L}_5, \mathcal{L}_6) \stackrel{\text{def}}{=} \overline{H}_{\mathcal{L}_3, \mathcal{L}_4}^{\mathcal{L}_2, \mathcal{L}_1}(\mathcal{L}_6) \circ C_{\mathcal{L}_1, \mathcal{L}_2, \mathcal{L}_3, \mathcal{L}_4} \circ H_{\mathcal{L}_2, \mathcal{L}_3}^{\mathcal{L}_1, \mathcal{L}_4}(\mathcal{L}_5) \\ : V_{\mathcal{L}_1, \mathcal{L}_2, \overline{\mathcal{L}_5}} \otimes V_{\mathcal{L}_3, \mathcal{L}_4, \mathcal{L}_5} \rightarrow V_{\mathcal{L}_2, \mathcal{L}_3, \overline{\mathcal{L}_6}} \otimes V_{\mathcal{L}_4, \mathcal{L}_1, \mathcal{L}_6} \quad (3.9)$$

Which fits the relation

$$H_{\mathcal{L}_2, \mathcal{L}_3}^{\mathcal{L}_1, \mathcal{L}_4}(\mathcal{L}_5) = \sum_{\mathcal{L}_6} C_{\mathcal{L}_1, \mathcal{L}_2, \mathcal{L}_3, \mathcal{L}_4}^{-1} \circ H_{\mathcal{L}_3, \mathcal{L}_4}^{\mathcal{L}_2, \mathcal{L}_1}(\mathcal{L}_6) \circ K_{\mathcal{L}_2, \mathcal{L}_3}^{\mathcal{L}_1, \mathcal{L}_4}(\mathcal{L}_5, \mathcal{L}_6) \quad (3.10)$$

This relation is called the H-junction crossing relation, and $K_{\mathcal{L}_2, \mathcal{L}_3}^{\mathcal{L}_1, \mathcal{L}_4}(\mathcal{L}_5, \mathcal{L}_6)$ is called the H-junction crossing kernel. The relation can be illustrated in Fig.12

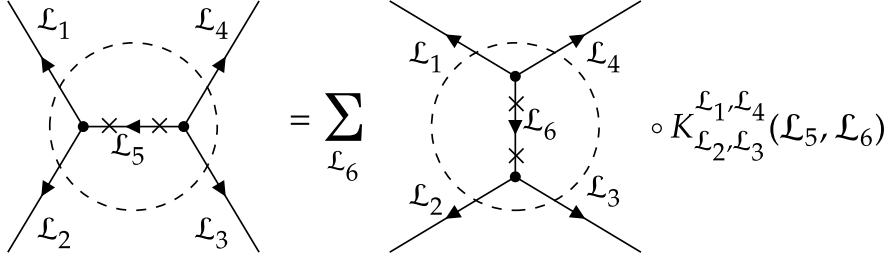


Figure 12: The H-junction crossing relation. The map $H_{\mathcal{L}_2, \mathcal{L}_3}^{\mathcal{L}_1, \mathcal{L}_4}(\mathcal{L}_5)$ is represented as the H-junction diagram. Note that the H-junction in the RHS is rotated 90 degrees, which corresponds to the permutation $C_{\mathcal{L}_1, \mathcal{L}_2, \mathcal{L}_3, \mathcal{L}_4}^{-1}$ that change the last leg. It can be seen that the crossing relation is the relation between 12-34 channel H-junctions and 23-41 channel ones.

Now we have obtained the relation between different channels of a graph with four external TDLs. A natural generalization is the case for five external TDLs, where we can apply the H-junction crossing relation multiple times and obtain the same graph in two different ways, which will be shown later in Fig.14. The corresponding self-consistency relation is called the Pentagon Identity.

However, when using the H-junction crossing kernel $K_{\mathcal{L}_2, \mathcal{L}_3}^{\mathcal{L}_1, \mathcal{L}_4}(\mathcal{L}_5, \mathcal{L}_6)$ defined above to describe this identity, the equation involves many extra cyclic permutation maps. In order to avoid this complexity, we define the permuted H-junction crossing kernel

$$F_{\mathcal{L}_2, \mathcal{L}_3}^{\mathcal{L}_1, \mathcal{L}_4}(\mathcal{L}_5, \mathcal{L}_6) \stackrel{\text{def}}{=} C_{\mathcal{L}_4, \mathcal{L}_1, \mathcal{L}_6} \circ K_{\mathcal{L}_2, \mathcal{L}_3}^{\mathcal{L}_1, \mathcal{L}_4}(\mathcal{L}_5, \mathcal{L}_6) \circ C_{\mathcal{L}_5, \mathcal{L}_3, \mathcal{L}_4} \\ : V_{\mathcal{L}_1, \mathcal{L}_2, \overline{\mathcal{L}_5}} \otimes V_{\mathcal{L}_5, \mathcal{L}_3, \mathcal{L}_4} \rightarrow V_{\mathcal{L}_2, \mathcal{L}_3, \overline{\mathcal{L}_6}} \otimes V_{\mathcal{L}_1, \mathcal{L}_6, \mathcal{L}_4} \quad (3.11)$$

which fits a permuted H-junction crossing relation

$$H_{\mathcal{L}_2, \mathcal{L}_3}^{\mathcal{L}_1, \mathcal{L}_4}(\mathcal{L}_5) \circ C_{\mathcal{L}_5, \mathcal{L}_3, \mathcal{L}_4} = \sum_{\mathcal{L}_6} C_{\mathcal{L}_1, \mathcal{L}_2, \mathcal{L}_3, \mathcal{L}_4}^{-1} \circ H_{\mathcal{L}_3, \mathcal{L}_4}^{\mathcal{L}_2, \mathcal{L}_1}(\mathcal{L}_6) \circ C_{\mathcal{L}_4, \mathcal{L}_1, \mathcal{L}_6}^{-1} \circ F_{\mathcal{L}_2, \mathcal{L}_3}^{\mathcal{L}_1, \mathcal{L}_4}(\mathcal{L}_5, \mathcal{L}_6) \quad (3.12)$$

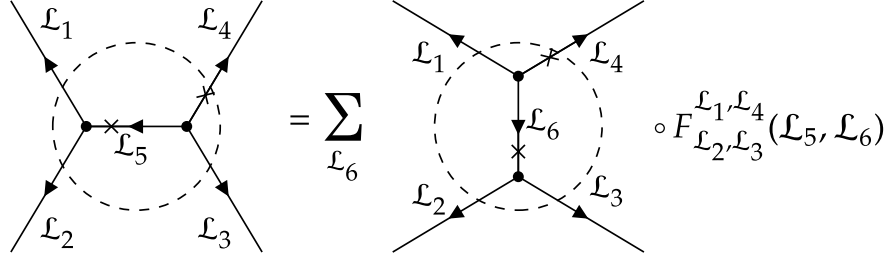


Figure 13: Illustration of permuted H-crossing relation. Note that LHS is a map from $V_{\mathcal{L}_1, \mathcal{L}_2, \overline{\mathcal{L}}_5} \otimes V_{\mathcal{L}_5, \mathcal{L}_3, \mathcal{L}_4}$ to $V_{\mathcal{L}_1, \mathcal{L}_2, \mathcal{L}_3, \mathcal{L}_4}$, which equals $H_{\mathcal{L}_2, \mathcal{L}_3}^{\mathcal{L}_1, \mathcal{L}_4}(\mathcal{L}_5) \circ C_{\mathcal{L}_5, \mathcal{L}_3, \mathcal{L}_4}$. The graph in the RHS is a map from $V_{\mathcal{L}_2, \mathcal{L}_3, \overline{\mathcal{L}}_6} \otimes V_{\mathcal{L}_1, \mathcal{L}_6, \mathcal{L}_4}$ to $V_{\mathcal{L}_1, \mathcal{L}_2, \mathcal{L}_3, \mathcal{L}_4}$, which equals $C_{\mathcal{L}_1, \mathcal{L}_2, \mathcal{L}_3, \mathcal{L}_4}^{-1} \circ H_{\mathcal{L}_3, \mathcal{L}_4}^{\mathcal{L}_2, \mathcal{L}_1}(\mathcal{L}_6) \circ C_{\mathcal{L}_4, \mathcal{L}_1, \mathcal{L}_6}^{-1}$

that can be illustrated in Fig.13

We permute the TDLs as in Fig.14, and obtain the Pentagon identity.

$$F_{j_2, k'_2}^{j_1, j_5}(k_1, k_3) \circ F_{j_3, j_4}^{k_1, j_5}(k_2, k'_2) = \sum_{k'_1} F_{j_3, j_4}^{j_2, \overline{k}_3}(k'_1, k'_2) \circ F_{k'_1, j_4}^{j_1, j_5}(k_2, k_3) \circ F_{j_2, j_3}^{j_1, \overline{k}_2}(k_1, k'_1) \quad (3.13)$$

Note that in (3.13) there is no summation $\sum_{k'_2} \sum_{k_3}$ because they occur on both sides and thus can be dropped. This identity is exactly the same as the one obtained through pure mathematical approaches in fusion algebra.

3.2.2 Conditions for Vacuum expectation value $\langle \mathcal{L} \rangle$ and twisted Hilbert space $\mathcal{H}_{\mathcal{L}}$

Remember that we obtain (3.8) through modular covariance. Let \mathcal{L}_2 be I , we have

$$\text{Tr} \left(\widehat{\mathcal{L}} \tilde{q}^{L_0 - \frac{c}{24}} \bar{\tilde{q}}^{\overline{L}_0 - \frac{c}{24}} \right) = \text{Tr}_{\mathcal{H}_{\mathcal{L}}} \left(q^{L_0 - \frac{c}{24}} \bar{q}^{\overline{L}_0 - \frac{c}{24}} \right) \quad (3.14)$$

where $\tilde{\tau} = -1/\tau$. Let $\tilde{\tau} \rightarrow i\infty$ i.e. $\tau \rightarrow 0i$, then LHS becomes only $\langle 0 | \widehat{\mathcal{L}} | 0 \rangle \tilde{q}^{-\frac{c}{12}} = \langle \mathcal{L} \rangle e^{2\pi \frac{i}{\tau} \cdot \frac{c}{12}}$. Thus, we have

$$\langle \mathcal{L} \rangle = \lim_{t \rightarrow 0} e^{-2\pi \frac{1}{t} \cdot \frac{c}{12}} \cdot \text{Tr}_{\mathcal{H}_{\mathcal{L}}} \left(e^{-2\pi t(L_0 + \overline{L}_0 - \frac{c}{24})} \right) \geq 0 \quad (3.15)$$

Also, setting all TDLs to spatial, the fusion rule (3.1) tells us that

$$\text{Tr} \left(\widehat{\mathcal{L}}_a \widehat{\mathcal{L}}_b q^{L_0 - \frac{c}{24}} \bar{q}^{\overline{L}_0 - \frac{c}{24}} \right) = \sum_c N_{ab}^c \text{Tr} \left(\widehat{\mathcal{L}}_c q^{L_0 - \frac{c}{24}} \bar{q}^{\overline{L}_0 - \frac{c}{24}} \right) \quad (3.16)$$

Similarly, taking $\tau \rightarrow i\infty$, we have

$$\langle 0 | \widehat{\mathcal{L}}_a \widehat{\mathcal{L}}_b | 0 \rangle = \sum_c N_{ab}^c \langle 0 | \widehat{\mathcal{L}}_c | 0 \rangle \quad (3.17)$$

then, by locality and $\widehat{\mathcal{L}} | 0 \rangle = \langle \mathcal{L} | 0 \rangle$, we have

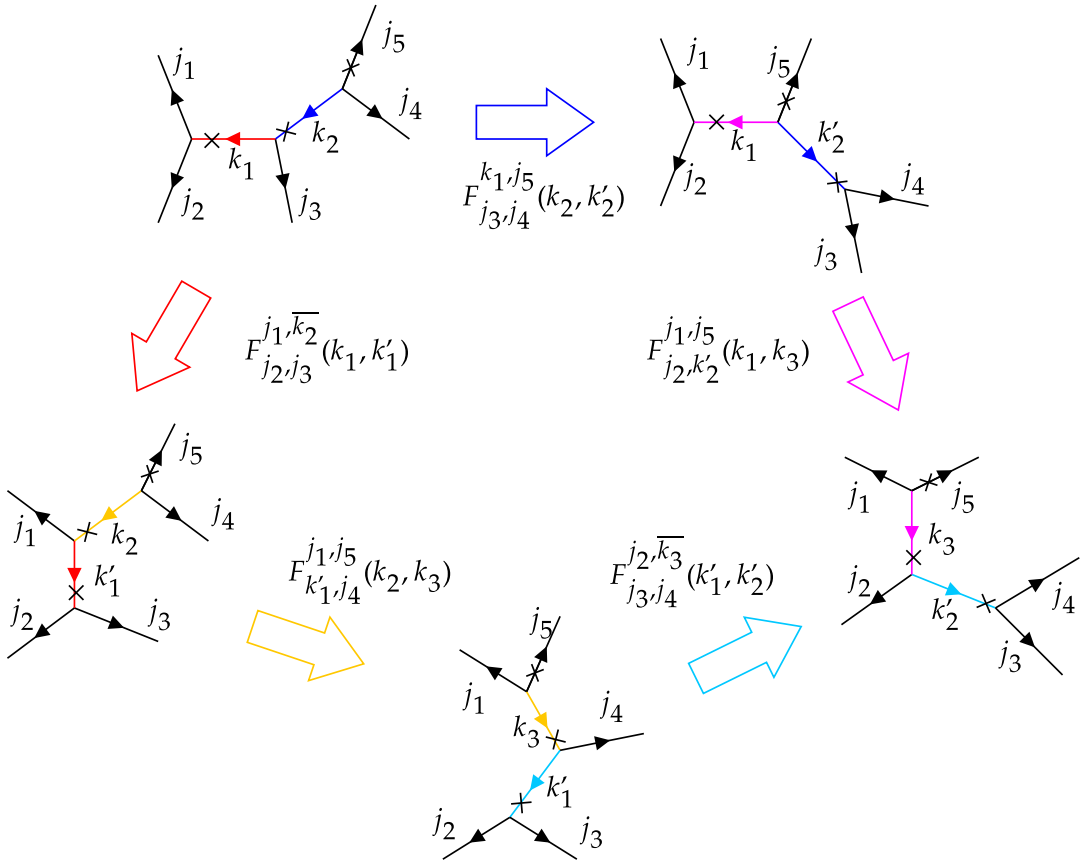


Figure 14: Illustration of Pentagon Identity. TDLs marked j_i are external ones crossing the boundaries while TDLs marked k_i are internal ones with junction vectors on both ends. The colored line marks the patch where we apply the H-junction crossing relation to relate different graphs. For example, the H-junction with k_1 in the middle is related to one with k'_1 through crossing kernel $F_{j_2,j_3}^{j_1,k_2}(k_1,k'_1)$. The lower right graph can be obtained by two moves on k_1 and k_2 , or three moves on k_2, k_1 and k'_2 . The fact that these two paths lead to the same result produces the Pentagon Identity.

$$\langle \mathcal{L}_a \rangle \langle \mathcal{L}_b \rangle = \sum_c N_{ab}^c \langle \mathcal{L}_c \rangle \quad (3.18)$$

which is a general condition for $\langle \mathcal{L} \rangle$. This is exactly the same condition as the one for quantum dimension in the fusion algebra.

Furthermore, in the next chapter, we will show that N_{ab}^c are all positive integers. In compact CFT, we expect \mathcal{L} to be bounded below by a positive number. Then, all $\langle \mathcal{L} \rangle$ should fit

$$\langle \mathcal{L} \rangle \geq 1 \quad (3.19)$$

so that any \mathcal{L}^n does not go to zero. Together with (3.18), one finds that for invertible TDLs, $\langle \mathcal{L} \rangle = \langle \overline{\mathcal{L}} \rangle = 1$ while for non-invertible ones, $\langle \mathcal{L} \rangle > 1$. Inserting back to (3.15), this condition also requires that

$$\mathcal{H}_{\mathcal{L}} \neq \emptyset \quad (3.20)$$

3.2.3 Fusion Coefficient

Similar to obtaining (3.16), by setting all TDLs to temporal and multiplying by $\overline{\mathcal{L}_c}$ on both sides, we have

$$\begin{aligned} \text{Tr}_{\mathcal{H}_{\mathcal{L}_a, \mathcal{L}_b, \overline{\mathcal{L}_c}}} \left(q^{L_0 - \frac{c}{24}} \bar{q}^{\overline{L}_0 - \frac{c}{24}} \right) &= N_{ab}^c \cdot \text{Tr}_{\mathcal{H}} \left(q^{L_0 - \frac{c}{24}} \bar{q}^{\overline{L}_0 - \frac{c}{24}} \right) \\ &\quad + \sum_d \#_d \text{Tr}_{\mathcal{H}_{\mathcal{L}_d}} \left(q^{L_0 - \frac{c}{24}} \bar{q}^{\overline{L}_0 - \frac{c}{24}} \right) \end{aligned} \quad (3.21)$$

The first term on the RHS comes from $\mathcal{L}_c \overline{\mathcal{L}_c}$, while the second term includes all the contributions with non-identity TDLs, where $\#_d$ are some constants produced by fusion rules. Taking $\tau \rightarrow i\infty$, we pick contribution from $(0, 0)$ states, i.e., states in the junction vector space V . Recall that $V_{\mathcal{L}_d}$ is empty, then

$$\dim_{\mathbb{C}} V_{\mathcal{L}_a, \mathcal{L}_b, \overline{\mathcal{L}_c}} = N_{ab}^c \quad (3.22)$$

A similar process produces

$$\dim_{\mathbb{C}} V_{\mathcal{L}, \overline{\mathcal{L}}} = 1 \quad (3.23)$$

3.3 Isotopy anomaly

The OPE of the energy-momentum tensor $T(z)$ and $\overline{T}(\bar{z})$ with TDL \mathcal{L} contains a contact term [26] of the form $T(x + iy) \sim i\alpha_{\mathcal{L}} \partial_y \delta(y)$, where \mathcal{L} is extended along $y \stackrel{\text{def}}{=} \text{Im } z = 0$ on the plane. As a result, when \mathcal{L} is deformed to sweep past a region D , its correlation functional may change by a phase factor

$$\exp\left(\frac{i\alpha_{\mathcal{L}}}{4\pi}\int_D d^2\sigma\sqrt{g}R(g)\right) \quad (3.24)$$

where g is the metric and $R(g)$ is the scalar curvature. (3.24) is the only possible form of the isotopy anomaly that is compatible with locality and conformal invariance. The coefficient $\alpha_{\mathcal{L}}$ fits $\alpha_{\mathcal{L}} = -\alpha_{\bar{\mathcal{L}}}$.

Recall that the vacuum expectation value $\langle \mathcal{L} \rangle$ is defined on the cylinder with $|0\rangle$ inserted on both ends, which can also be interpreted as the expectation value of \mathcal{L} on the equator of S^2 . This suggests that $\langle \mathcal{L} \rangle$ is different from the expectation value of an empty counterclockwise \mathcal{L} loop on the plane, which we denote as $R(\mathcal{L})$. By contracting \mathcal{L} on the equator to the north pole or south pole, we find that

$$R(\mathcal{L}) = e^{i\alpha_{\mathcal{L}}} \langle \mathcal{L} \rangle, \quad R(\bar{\mathcal{L}}) = e^{-i\alpha_{\mathcal{L}}} \langle \mathcal{L} \rangle \quad (3.25)$$

This difference can be canceled with the help of the Gauss-Bonnet Theorem by including in the definition of TDL \mathcal{L} on the plane a factor

$$\exp\left(\frac{i\alpha_{\mathcal{L}}}{2\pi}\int_{\mathcal{L}} ds K\right) \quad (3.26)$$

where K is the curvature of the TDL \mathcal{L} . However, this factor may also introduce extra phases in junction vectors or defect operators, and thus modify the crossing kernel by some factor while preserving the Pentagon identity. As an example, consider the junction vector space $V_{\mathcal{L},\bar{\mathcal{L}},I}$, which should be trivial, as in Fig.15. But (3.26) introduces a phase in the RHS of Fig.15, in order to maintain the equivalence, the junction vector in $V_{\mathcal{L},\bar{\mathcal{L}},I}$ should also multiply the same factor.

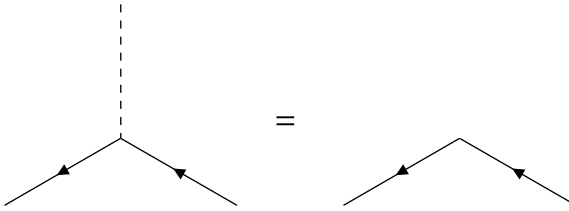


Figure 15: A junction vector in trivial junction vector space $V_{\mathcal{L},\bar{\mathcal{L}},I}$ should be removable because it can be added everywhere in a graph. When a factor is multiplied in the definition of \mathcal{L} , there appears an extra phase on the RHS, suggesting that the same phase should appear on the LHS.

Furthermore, (3.26) does not work for $\mathcal{L} = \bar{\mathcal{L}}$ on the plane because it violates $R(\mathcal{L}) = R(\bar{\mathcal{L}})$. In this case, either there is an orientation-reverse anomaly that on a curved surface, correlation functions involving \mathcal{L} differ by a phase depending on the choice of orientation, or $\alpha_{\mathcal{L}} = \pi$ and $R(\mathcal{L}) = -\langle \mathcal{L} \rangle$, which is an isotopy anomaly that cannot be canceled.

4 Application of invertible lines

4.1 Invertible TDLs and 't Hooft anomaly

As we have mentioned before, a global symmetry group element $g \in G$ corresponds to an invertible TDL \mathcal{L}_g that fits $\widehat{\mathcal{L}}_g |\phi\rangle = \hat{g} |\phi\rangle$, $\mathcal{L}_{g_1} \mathcal{L}_{g_2} = \mathcal{L}_{g_1 g_2}$, $\overline{\mathcal{L}_g} = \mathcal{L}_{g^{-1}}$, $\langle \mathcal{L}_g \rangle = 1$. Furthermore, applying the equation for the fusion coefficient (3.22), we know that $V_{\mathcal{L}_{g_1}, \mathcal{L}_{g_2}, \mathcal{L}_{g_3}} = \mathbb{C}$ when $\mathcal{L}_{g_1} \mathcal{L}_{g_2} = \mathcal{L}_{g_3}^{-1}$, and it is trivial otherwise.

The 't Hooft anomaly can be described by the phase in the H-junction crossing kernel $F_{j_2, j_3}^{j_1, j_4}(k_1, k'_1)$ [27]. Taking into account the properties of invertible TDLs, the junction vector in $V_{\mathcal{L}_{g_1}, \mathcal{L}_{g_2}, \overline{\mathcal{L}_{g_1 g_2}}}$ should have a unit norm, and the H-junction crossing kernel becomes

$$F_{g_2, g_3}^{g_1, \overline{g_1 g_2 g_3}}(g_1 g_2, g_2 g_3) = e^{i\theta(g_1, g_2, g_3)} \quad (4.1)$$

The phase θ can be interpreted as a map: $G^3 \rightarrow U(1)$. The Pentagon identity (3.13) becomes

$$\begin{aligned} & F_{g_2, g_3, g_4}^{g_1, \overline{g_1 g_2 g_3 g_4}}(g_1 g_2, g_2 g_3 g_4) \circ F_{g_3, g_4}^{g_1 g_2, \overline{g_1 g_2 g_3 g_4}}(g_1 g_2 g_3, g_3 g_4) \\ &= F_{g_3, g_4}^{g_2, \overline{g_2 g_3 g_4}}(g_2 g_3, g_3 g_4) \circ F_{g_2 g_3, g_4}^{g_1, \overline{g_1 g_2 g_3 g_4}}(g_1 g_2 g_3, g_2 g_3 g_4) \circ F_{g_2, g_3}^{g_1, \overline{g_1 g_2 g_3}}(g_1 g_2, g_2 g_3) \end{aligned} \quad (4.2)$$

which boils down to

$$\theta(g_1, g_2, g_3 g_4) + \theta(g_1 g_2, g_3, g_4) = \theta(g_2, g_3, g_4) + \theta(g_1, g_2 g_3, g_4) + \theta(g_1, g_2, g_3) \quad (4.3)$$

Rewrite this equation as

$$g_1 \cdot \theta(g_2, g_3, g_4) - \theta(g_1 g_2, g_3, g_4) + \theta(g_1, g_2 g_3, g_4) - \theta(g_1, g_2, g_3 g_4) + \theta(g_1, g_2, g_3) = 0 \quad (4.4)$$

where G acts on $U(1)$ trivially, i.e., $g \cdot \theta = \theta$.

Define a map $d^n : (G^{n-1} \rightarrow U(1)) \rightarrow (G^n \rightarrow U(1))$ that acts on $\theta : G^{n-1} \rightarrow U(1)$ as

$$\begin{aligned} & (d^n \circ \theta)(g_1, g_2, \dots, g_n) \\ &= g_1 \cdot \theta(g_2, \dots, g_n) + \sum_{i=1}^{n-1} (-1)^i \cdot \theta(g_1, \dots, g_{i-1} g_i, \dots, g_n) + \theta(g_1, \dots, g_{n-1}) \end{aligned} \quad (4.5)$$

A critical property of d^n is that $d^{n+1} \circ d^n = 0$. Using d^n , equation (4.4) is just

$$(d^4 \circ \theta)(g_1, g_2, g_3, g_4) = 0 \quad (4.6)$$

Apart from equation (4.6), we also require that when a general shift $e^{i\phi(g_1, g_2)}$ is performed on the junction vector in $V_{g_1, g_2, \overline{g_1 g_2}}$, the new θ phase is equivalent to the original. Remember that $F_{g_2, g_3}^{g_1, \overline{g_1 g_2 g_3}}(g_1 g_2, g_2 g_3)$ is a map from $V_{g_1, g_2, \overline{g_1 g_2}} \otimes V_{g_1 g_2, g_3, \overline{g_1 g_2 g_3}}$ to $V_{g_2, g_3, \overline{g_2 g_3}} \otimes V_{g_1, g_2 g_3, \overline{g_1 g_2 g_3}}$, then a shift $e^{i\phi(g_1, g_2)}$ means

$$\theta(g_1, g_2, g_3) \rightarrow \theta(g_1, g_2, g_3) - \phi(g_1, g_2) - \phi(g_1 g_2, g_3) + \phi(g_2, g_3) + \phi(g_1, g_2 g_3) \quad (4.7)$$

which is just

$$\theta \rightarrow \theta + d^3 \circ \phi \quad (4.8)$$

Combining equation (4.6) and the equivalence under (4.8), the remaining non-equivalent phases form a group **Ker** $d^4/\text{Im } d^3$, which is exactly $H^3(G, U(1))$ in the group cohomology language. For the specific case of $G = \mathbb{Z}_n$, we also know that $H^3(\mathbb{Z}_n, U(1)) = \mathbb{Z}_n$ from mathematics. The non-anomalous case corresponds to the trivial element in this group, where all phases can be canceled under the equivalence relation.

If the global symmetry group G is free of an 't Hooft anomaly, i.e., take the trivial element in $H^3(G, U(1))$, we can choose

$$d^3 \circ \phi(g_1, g_2) = 0 \quad (4.9)$$

so that $\theta(g_1, g_2, g_3) = 0$. Apart from that, a general shift $e^{i\alpha(g)}$ in the trivial junction vector space $V_{g, \overline{g}, I}$ should keep $\phi(g_1, g_2)$ equivalent. $\phi(g_1, g_2)$ is the phase in $V_{g_1, g_2, \overline{g_1 g_2}}$, then the equivalence relation is

$$\begin{aligned} \phi(g_1, g_2) &\sim \phi(g_1, g_2) + \alpha(g_1) + \alpha(g_2) + \alpha(\overline{g_1 g_2}) \\ &\sim \phi(g_1, g_2) + \alpha(g_1) + \alpha(g_2) - \alpha(g_1 g_2) \\ &\sim \phi(g_1, g_2) + (d^2 \circ \alpha)(g_1, g_2) \end{aligned} \quad (4.10)$$

Combining equation (4.9) and the equivalence relation (4.10), the remaining non-equivalent phases are **Ker** $d^3/\text{Im } d^2 = H^2(G, U(1))$. These non-equivalent phases actually correspond to the non-equivalent orbifolds constructed by the 't Hooft anomaly free G , where the space of local operators is the G -invariant projection of $\bigoplus_{g \in G} \mathcal{H}_g$. $H^2(G, U(1))$ is also known as the classification of discrete torsions [28, 29].

4.2 Cyclic permutation map and spin selection rule

Given an order- n element g of a general global symmetry group G , that is, $g^n = 1$, the presence of the 't Hooft anomaly will lead to a spin selection rule on the defect operators in \mathcal{H}_g . The process involves the cylinder cyclic permutation map \tilde{C} acting on the n -way junction vector space $V_{g, \dots, g}$, which connects the i -th \mathcal{L}_g to

the $i + 1$ -th on the cylinder, as shown in Fig.16. Note that the Hilbert space on the bottom and top of the cylinder should be restricted to $V_{g,\dots,g} \subset \mathcal{H}_{g,\dots,g}$. Since \tilde{C}^n is the identity map and $V_{g,\dots,g} = \mathbb{C}$, we must have $\tilde{C} = e^{i2\pi \frac{k}{n}}$ ($k \in \mathbb{Z}$).

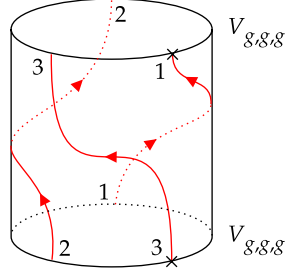


Figure 16: The cylinder cyclic permutation map $\tilde{C} : V_{1,2,3} \rightarrow V_{2,3,1}$

\tilde{C} differs from the cyclic permutation map C by the phase $e^{i\alpha_g}$ when the isotopy anomaly is present. This can be seen by the isotopy between the two maps, as shown in Fig.17, where the sweeping through the upper hemisphere produces the phase $e^{i\alpha_g}$ according to (3.24). Alternatively, \tilde{C} can also be achieved by several steps involving the H-junction crossing kernel $F_{\bar{g},g}^{g,\bar{g}}$ and cyclic permutation C , as shown in Fig.18. The two approaches indicate that the phase of \tilde{C} precisely corresponds to elements in $H^3(G, U(1))$.

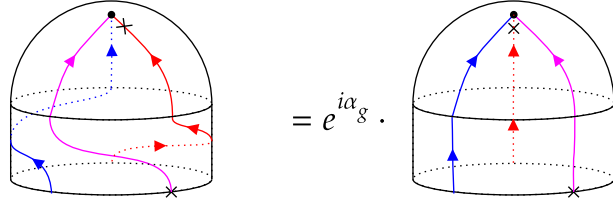


Figure 17: The isotopy between \tilde{C} (left) and C (right) involves \mathcal{L}_g sweeping through a hemisphere.

Now we derive a spin selection rule on \mathcal{H}_g . Consider the effect of n times of T transformation on the partition function Z_g , where the modular covariance property plays a role, but an extra phase may occur due to the anomaly:

$$T^n Z_g(\tau) = \gamma Z_g(\tau) \quad (4.11)$$

In order to obtain γ , we perform an S transformation on both sides of (4.11) and restrict the Hilbert space to $V_{g,\dots,g}$. This process can be illustrated in Fig.19 and produces

$$\tilde{C} = \gamma \quad (4.12)$$

Inserting back to (4.11) and writing out the partition function after T transformation, we have

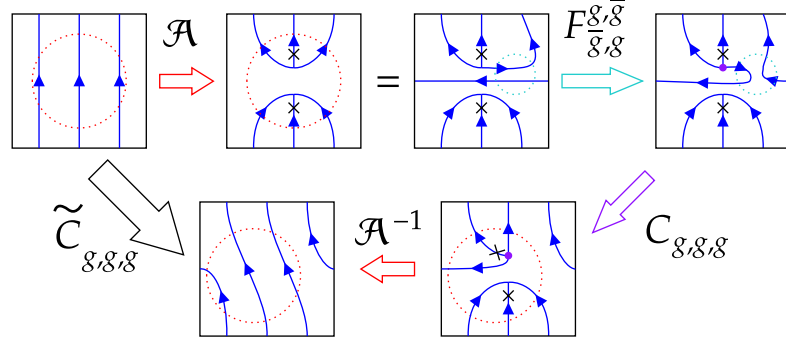


Figure 18: The illustration of $\tilde{C} = F_{\bar{g},g}^{g,\bar{g}} \cdot C$ for $n = 3$ on a torus. The equality on the first line comes from the fact that g acts trivially on the ground state. The map \mathcal{A} is canceled by the inverse of itself.

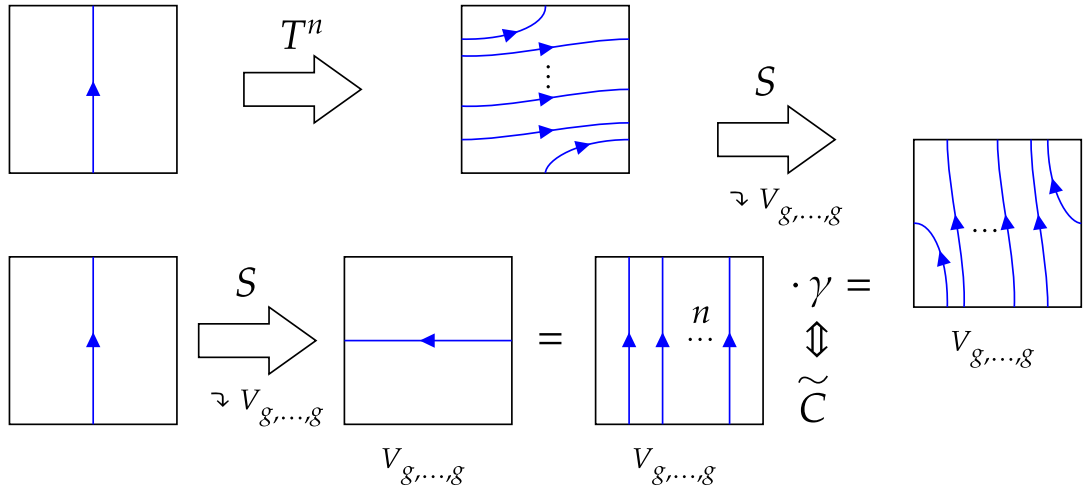


Figure 19: The illustration of $\gamma = \tilde{C}$. Starting from the partition function Z_g , (4.11) tells us that $ST^n Z_g = SZ_g \cdot \gamma$, while it can be seen from the illustration that $ST^n Z_g = \tilde{C}SZ_g$ after restriction to the junction vector space $V_{g,...,g}$. The equation on the second line holds because g acts trivially on $V_{g,...,g}$, and $g^n = I$. The act of \tilde{C} on the graph is just the same as Fig.16

$$\text{Tr}_{\mathcal{H}_g} \left(e^{i2\pi n(L_0 - \bar{L}_0)} q^{L_0 - c/24} \bar{q}^{\bar{L}_0 - c/24} \right) = \tilde{C} \text{Tr}_{\mathcal{H}_g} \left(q^{L_0 - c/24} \bar{q}^{\bar{L}_0 - c/24} \right) \quad (4.13)$$

Remember $\tilde{C} = e^{i2\pi \frac{k}{n}}$, thus

$$h - \bar{h} \in \frac{\mathbb{Z}}{n} + \frac{k}{n^2} \quad (4.14)$$

The k here actually labels a class in $H^3(G, U(1))$ that represents the 't Hooft anomaly. For $G = \mathbb{Z}_n$, for example, $k \in \mathbb{Z}_n = H^3(\mathbb{Z}_n, U(1))$.

4.2.1 Example: $U(1)$ rotation in free boson on S^1

Let us consider the explicit example of the compact free boson CFT on S^1 , whose action is

$$S = \frac{1}{2\pi} \int d^2z \partial X \cdot \bar{\partial} X \quad (4.15)$$

which is invariant under $X(z, \bar{z}) \rightarrow X(z, \bar{z}) + \epsilon$. The equation of motion of X permits the decomposition $X(z, \bar{z}) = X_L(z) + X_R(\bar{z})$, then the Noether current is $\bar{j} = -\bar{\partial}X_R$ for $X_L \rightarrow X_L + \epsilon$ and $j = -\partial X_L$ for $X_R \rightarrow X_R + \epsilon$. OPE of X is $X(z, \bar{z})X(0, 0) \sim -\frac{1}{2}\ln|z^2|$. The compactification of X on S^1 means $X \sim X + 2\pi Rm$, where we set $R = 1$ so that the partition function is self-dual.

The invertible TDL \mathcal{L}_α corresponding to the shift $X_L \rightarrow X_L + \alpha$ is

$$\mathcal{L}_\alpha = : \exp \left(-2\alpha \oint \frac{dz}{2\pi i} \partial X(z) \right) : \quad (4.16)$$

This definition makes $R(\mathcal{L}_\alpha) = 1$, which means no isotopy anomaly. In the self-dual case, $\mathcal{L}_{2\pi} = I$. The ground state in twisted Hilbert space $\mathcal{H}_{\mathcal{L}_\alpha}$ can be written as

$$\Psi_\alpha(z) = : \exp \left(i \frac{\alpha}{\pi} X_L(z) \right) : \quad (4.17)$$

whose conformal weight is $(\frac{\alpha^2}{4\pi^2}, 0)$. We pick TDLs $\mathcal{L}_0, \mathcal{L}_{\frac{2}{3}\pi}, \mathcal{L}_{-\frac{2}{3}\pi}$ that form the fusion ring \mathbb{Z}_3 . Consider a graph of three $\Psi_{\frac{2}{3}\pi}(z)$ joining at a 3-way junction of $\mathcal{L}_{\frac{2}{3}\pi}$, the OPE takes the form

$$\Psi_{\frac{2}{3}\pi}(z_1)\Psi_{\frac{2}{3}\pi}(z_2)\Psi_{\frac{2}{3}\pi}(z_3) = (z_{12}z_{23}z_{31})^{-\frac{2}{9}}\Psi_{2\pi}\left(\frac{z_1 + z_2 + z_3}{3}\right) + \dots \quad (4.18)$$

where $\Psi_{2\pi}$ has weight $(1, 0)$, and the omitted terms are of higher weights. The $\Psi_{\frac{2}{3}\pi}$ has weight $(\frac{1}{9}, 0)$, which satisfies the spin selection rule (4.14) for $n = 3, k = 1$. We take $z_j = ze^{i\frac{2}{3}\pi j}$ for simplicity in the following analysis. The effect of the cyclic permutation map on the junction has the same effect as a $\frac{2}{3}\pi$ rotation: $z \rightarrow ze^{i\frac{2}{3}\pi}$ on the $\Psi_{2\pi}(0)$ on the RHS of the OPE, which results in a phase $e^{-i\frac{2}{3}\pi}$. Alternatively, the cyclic permutation map can be realized by a continuous deformation followed by a $\frac{2}{3}\pi$ rotation: $z \rightarrow ze^{i\frac{2}{3}\pi}$ on all three $\Psi_{\frac{2}{3}\pi}$, as depicted in

Fig.20. The continuous deformation brings $z_1 \rightarrow z_2, z_2 \rightarrow z_3, z_3 \rightarrow z_1$, resulting in $z_{12} \rightarrow z_{12} e^{i\frac{2}{3}\pi}$ and thus produces a $e^{-i2\pi \cdot \frac{2}{9}}$ due to the $(z_{12} z_{23} z_{31})^{-\frac{2}{9}}$ term on the RHS. The rotation produces a total $e^{-i2\pi \cdot \frac{1}{9}}$ phase. The final net effect is again the phase $e^{-i\frac{2}{3}\pi}$. This is exactly the \tilde{C} we discussed before.

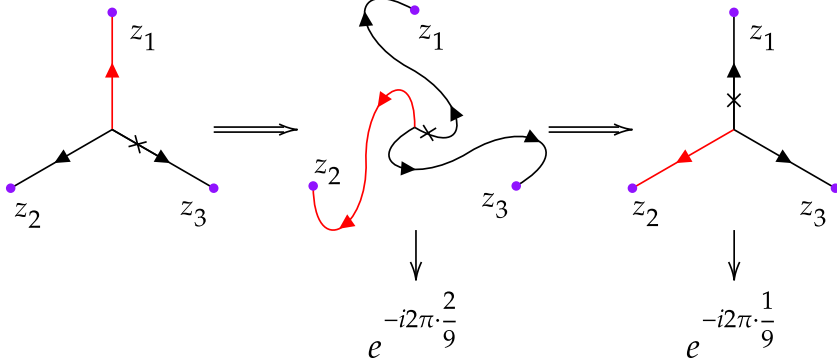


Figure 20: An alternative way to realize the cyclic permutation map. The colored line marks how the deformation is performed. As we can see, in the first step the angle at the endpoint of the lines is preserved, while in the second step they are rotated.

5 Topological defect lines in rational CFTs

In this section, we will discuss TDLs in rational conformal field theories (RCFTs), which are generally not invertible lines, and examine the example of the critical Ising model. We will also discuss the spin selection rule derived by crossing kernels involving the non-invertible TDLs.

5.1 The non-invertible TDL \mathcal{N} and the Tambara-Yamagami category

First, we introduce an important type of non-invertible TDL that plays a role in multiple RCFTs including the critical Ising model, tricritical Ising model, and three-state Potts model. In the sections before we have discussed the invertible TDLs corresponding to the global symmetry group G . Setting $G = \mathbb{Z}_n$, we can include a non-invertible TDL \mathcal{N} which fits the following fusion rule:

$$\begin{aligned} \mathcal{N}\mathcal{L}_g &= \mathcal{L}_g\mathcal{N} = \mathcal{N}, \quad \forall g \in \mathbb{Z}_n \\ \mathcal{N}^2 &= \sum_{g \in \mathbb{Z}_n} \mathcal{L}_g \end{aligned} \tag{5.1}$$

Note that $\overline{\mathcal{N}} = \mathcal{N}$. Such a fusion rule implies that \mathcal{N} annihilates any states with nontrivial \mathbb{Z}_n charge. It can also be derived from the fusion rule that $\langle \mathcal{N} \rangle = \sqrt{n}$,

therefore $v \in V_{\mathcal{N}, \mathcal{N}, I}$ has the norm $|v| = \sqrt[4]{n}$. By considering the process shown in Fig.21, we find that $F_{\mathcal{N}, g^k}^{g^m, \mathcal{N}}(\mathcal{N}, \mathcal{N}) = \left(F_{\mathcal{N}, g^k}^{g, \mathcal{N}}(\mathcal{N}, \mathcal{N})\right)^m$, and similar process gives $F_{\mathcal{N}, g^k}^{g^m, \mathcal{N}}(\mathcal{N}, \mathcal{N}) = \left(F_{\mathcal{N}, g}^{g, \mathcal{N}}(\mathcal{N}, \mathcal{N})\right)^{mk}$. We then have

$$F_{\mathcal{N}, g^k}^{g^m, \mathcal{N}}(\mathcal{N}, \mathcal{N}) = \omega^{mk} \quad (5.2)$$

where $\omega = e^{i \frac{2\pi}{n}}$ because $\mathbb{Z}_n \ni m \sim m + n$.

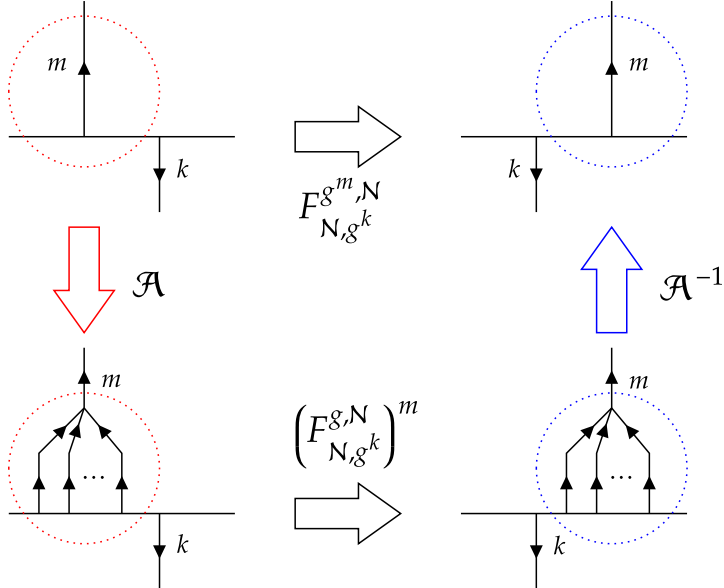


Figure 21: Illustration of $F_{\mathcal{N}, g^k}^{g^m, \mathcal{N}}(\mathcal{N}, \mathcal{N}) = \left(F_{\mathcal{N}, g^k}^{g, \mathcal{N}}(\mathcal{N}, \mathcal{N})\right)^m$. \mathcal{A} is some map that modifies the circled patch in the graph, whose effect is canceled by \mathcal{A}^{-1} in the end.

Similarly, we can have $F_{\mathcal{N}, \mathcal{N}}^{g^m, g^k}(g^m, g^k) = a\omega^{mk}$ but left with some constant a to be determined. The constant can be obtained through one of the Pentagon identities

$$F_{\mathcal{N}, I}^{\mathcal{N}, I}(I, \mathcal{N}) \circ F_{\mathcal{N}, \mathcal{N}}^{I, I}(\mathcal{N}, I) = \sum_{g^k} F_{\mathcal{N}, \mathcal{N}}^{g^m, g^k}(g^m, g^k) \circ F_{g^k, \mathcal{N}}^{\mathcal{N}, I}(\mathcal{N}, \mathcal{N}) \circ F_{\mathcal{N}, \mathcal{N}}^{\mathcal{N}, \mathcal{N}}(I, g^k) \quad (5.3)$$

which gives $n^2 a = 1 \Rightarrow a = \pm \frac{1}{\sqrt{n}}$, meaning that

$$F_{\mathcal{N}, \mathcal{N}}^{g^m, g^k}(g^m, g^k) = \pm \frac{1}{\sqrt{n}} \omega^{mk} \quad (5.4)$$

It can be checked that these results satisfy the whole set of Pentagon identities. Indeed, one can also derive the above results only from the Pentagon identities.

In fact, the TDL \mathcal{N} described above describes a duality between a 2d CFT \mathcal{T} with non-anomalous \mathbb{Z}_n symmetry and its \mathbb{Z}_n -orbifold CFT \mathcal{T}/\mathbb{Z}_n . In the critical Ising model where $G = \mathbb{Z}_2$, \mathcal{N} generalizes the order-disorder duality (Kramers-Wannier duality) [30]. As a rough image of this duality, consider the 8-way junction

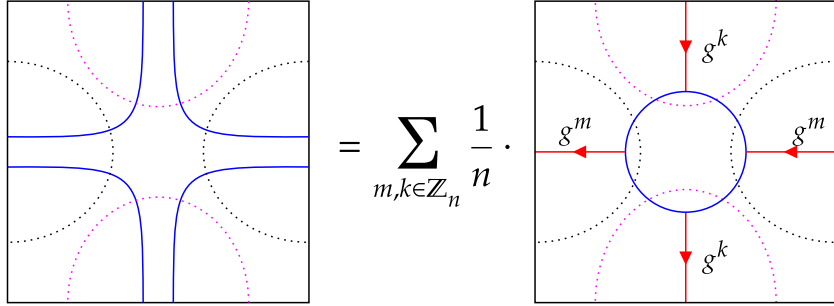


Figure 22: Fusing an 8-way junction of non-invertible \mathcal{N} (blue) into a 4-way junction of invertible TDLs (red) by crossing relation on the circled patches. Note that the graph is on a torus.

of \mathcal{N} on torus as shown in Fig.22, where we apply the crossing relation derived above to produce a summation of 4-way junctions of $\mathcal{L}_{g^k}, \mathcal{L}_{g^m}$'s. Note that we have chosen the + sign in the $F_{\mathcal{N},\mathcal{N}}^{\mathcal{N},\mathcal{N}}$ here. The equality in Fig.22 can be understood as an isomorphism between \mathcal{T} and \mathcal{T}/\mathbb{Z}_n , as the graph on the LHS can be shrunk to a contractible circle of \mathcal{N} , giving the torus partition function of \mathcal{T} times the expectation value of \mathcal{N} on the torus. On the RHS, summing over all the invertible lines $g \in \mathbb{Z}_n$ gives the torus partition function of the \mathcal{T}/\mathbb{Z}_n , again times the expectation value of \mathcal{N} on the torus. The equality between them then proves the equality between the torus partition functions of \mathcal{T} and \mathcal{T}/\mathbb{Z}_n .

The construction described above is a special case of the Tambara-Yamagami (TY) category [31], which allows the \mathbb{Z}_n group discussed above to be any abelian group, with \mathcal{N} obeying the same fusion rules (5.1). Our conclusion above can then be rephrased as follows: a 2d CFT \mathcal{T} with a non-anomalous abelian finite group global symmetry G is isomorphic to its G -orbifold theory \mathcal{T}/G if \mathcal{T} contains a TY extension of the G fusion category.

5.2 Verlinde lines

In an RCFT with diagonal modular invariance, there is a simple and explicit construction for a family of TDLs, known as the Verlinde lines, that commute with not only the Virasoro algebra but the entire (left and right) chiral vertex algebra of the RCFT. In fact, modular invariance constrains the Verlinde lines in a diagonal RCFT to be in one-to-one correspondence with the chiral vertex algebra primaries. The partition function of an RCFT takes the form

$$Z(\tau, \bar{\tau}) = \sum_{i,j} n_{i,j} \chi_i(\tau) \bar{\chi}_j(\bar{\tau}) \quad (5.5)$$

where $\chi_i(\tau)$ is the character of an irreducible representation of the chiral vertex algebra labeled by the index i , and $n_{ij} \in \mathbb{Z}^+$ is the degeneracy. The vacuum representation is labeled by 0. A diagonal CFT means that $n_{ij} = \delta_{ij}$. Under S

transformation, $\chi_i(\tau)$ becomes

$$\chi_i(-\frac{1}{\tau}) = \sum_j S_{ij} \chi_j(\tau) \quad (5.6)$$

where S_{ij} is unitary and symmetric. The fusion rule has the form

$$[i] \times [j] = \sum_k N_{ij}^k [k] \quad (5.7)$$

where $[i]$ denotes the operators in the i representation. The fusion coefficients $N_{ij}^k \in \mathbb{Z}^+$ should fit the Verlinde formula

$$N_{ij}^k = \sum_l \frac{S_{il} S_{jl} S_{kl}^*}{S_{0l}} \quad (5.8)$$

In diagonal CFT, the primary fields ϕ_k correspond to the irreducible representation k of the chiral vertex algebra. The Verlinde lines and the primary fields are in one-to-one correspondence and, therefore can be denoted as \mathcal{L}_k . It fits

$$\widehat{\mathcal{L}}_k |\phi_i\rangle = \frac{S_{ki}}{S_{0i}} |\phi_i\rangle \quad (5.9)$$

and it commutes with the whole chiral vertex algebra. From the modular S transformation of the torus character, we obtain the partition function of the $\mathcal{H}_{\mathcal{L}_k}$

$$Z_{\mathcal{L}_k}(\tau, \bar{\tau}) = \sum_{i,j} N_{ki}^j \chi_i(\tau) \bar{\chi}_j(\bar{\tau}) \quad (5.10)$$

which means $\mathcal{H}_{\mathcal{L}_k}$ consists of states in the representation i of the chiral vertex algebra and representation j of the anti-chiral vertex algebra, with degeneracy $N_{ki}^j \in \mathbb{Z}^+$. For $k = 0$, states in $\mathcal{H}_{\mathcal{L}_k}$ usually have $h - \bar{h} \notin \mathbb{Z}$.

The fusion rules of the Verlinde lines \mathcal{L}_k are the same as the chiral algebra primary operators in the RCFT

$$\mathcal{L}_i \mathcal{L}_j = \sum_k N_{ij}^k \mathcal{L}_k \quad (5.11)$$

Note that the Verlinde lines always generate a commutative fusion ring. Now we will study the Verlinde lines in the critical Ising model explicitly.

5.3 Ising model

The $c = \frac{1}{2}$ critical Ising model is the minimal model $\mathcal{M}_{3,4}$. It has three primary fields:

$$\mathbf{1}_{0,0}, \epsilon_{\frac{1}{2}, \frac{1}{2}}, \sigma_{\frac{1}{16}, \frac{1}{16}} \quad (5.12)$$

which are the identity, the energy density operator, and the spin field. Their fusion rules are

$$\epsilon \times \epsilon = 1, \quad \sigma \times \sigma = 1 + \epsilon, \quad \epsilon \times \sigma = \sigma \times \epsilon = \sigma \quad (5.13)$$

There are three simple Verlinde lines: the trivial line I , the \mathbb{Z}_2 invertible line η , and the \mathcal{N} line. Together they form a \mathbb{Z}_2 TY category, where the \mathcal{N} is the duality defect for the Kramers-Wannier duality. These TDLs act on the local primary operators with eigenvalues:

$$\begin{array}{ccc} 1 & \epsilon & \sigma \\ \eta : & 1 & 1 & -1 \\ \mathcal{N} : & \sqrt{2} & -\sqrt{2} & 0 \end{array} \quad (5.14)$$

and fusion rules

$$\eta^2 = I, \quad \mathcal{N}^2 = I + \eta, \quad \eta\mathcal{N} = \mathcal{N}\eta = \mathcal{N} \quad (5.15)$$

Note that $\mathcal{N} = \overline{N}$, $\eta = \overline{\eta}$. The defect Hilbert space $\mathcal{H}_\eta, \mathcal{H}_\mathcal{N}$ are determined by (5.10), and are spanned by the primaries:

$$\begin{aligned} \mathcal{H}_\eta : & \psi_{\frac{1}{2},0}, \bar{\psi}_{0,\frac{1}{2}}, \mu_{\frac{1}{16},\frac{1}{16}} \\ \mathcal{H}_\mathcal{N} : & s_{\frac{1}{16},0}, \bar{s}_{0,\frac{1}{16}}, \Lambda_{\frac{1}{16},\frac{1}{2}}, \bar{\Lambda}_{\frac{1}{2},\frac{1}{16}} \end{aligned} \quad (5.16)$$

where the η is just the disorder operator in the critical Ising model. Since the junction vector in $V_{\mathcal{N},\mathcal{N},I}$ has the norm $\sqrt[4]{2}$, we can choose $v \in V_{\mathcal{N},\mathcal{N},\eta}$ also has the norm $\sqrt[4]{2}$. Then the nontrivial crossing kernels are [32]

$$F_{\mathcal{N},\mathcal{N}}^{\mathcal{N},\mathcal{N}} = \begin{pmatrix} F_{\mathcal{N},\mathcal{N}}^{\mathcal{N},\mathcal{N}}(I,I) & F_{\mathcal{N},\mathcal{N}}^{\mathcal{N},\mathcal{N}}(I,\eta) \\ F_{\mathcal{N},\mathcal{N}}^{\mathcal{N},\mathcal{N}}(\eta,I) & F_{\mathcal{N},\mathcal{N}}^{\mathcal{N},\mathcal{N}}(\eta,\eta) \end{pmatrix} = \begin{pmatrix} \frac{1}{\sqrt{2}} & \frac{1}{\sqrt{2}} \\ \frac{1}{\sqrt{2}} & -\frac{1}{\sqrt{2}} \end{pmatrix}, \quad F_{\mathcal{N},\eta}^{\eta,\mathcal{N}} = -1 \quad (5.17)$$

as we have obtained in (5.4) and (5.2). Also, we can consider the effect of passing \mathcal{N} through σ , which may leave behind a defect state attached to a TDL η , as shown in Fig.23. The state can only be $a\mu_{\frac{1}{16},\frac{1}{16}} \in \mathcal{H}_\eta$ due to the preservation of conformal weights, where a is a coefficient to be determined. To determine a ,

Figure 23: Moving \mathcal{N} past σ should change σ to μ , which shows the order-disorder duality effect of \mathcal{N} . The $\frac{1}{\sqrt{2}}$ is the normalizing factor.

consider the graph of an \mathcal{N} loop circling two σ operators, as shown in Fig.24. By applying a partial fusion on the \mathcal{N} loop, one gets a vanishing term due to $\widehat{\mathcal{N}} \cdot \sigma = 0$ and a term with two $\widehat{\mathcal{N}} \cdot \sigma = a\mu$. We know the OPE of ϵ and μ are [25]

$$\epsilon(z, \bar{z})\epsilon(0, 0) = \frac{1}{|z|^{\frac{1}{4}}} + \frac{1}{2}|z|^{\frac{3}{4}}\epsilon(0, 0) + \dots \quad (5.18)$$

$$\mu(z, \bar{z})\mu(0, 0) = \frac{1}{|z|^{\frac{1}{4}}} - \frac{1}{2}|z|^{\frac{3}{4}}\epsilon(0, 0) + \dots \quad (5.19)$$

and $\hat{\mathcal{N}} \cdot I = \sqrt{2}I$, $\hat{\mathcal{N}} \cdot \epsilon = \sqrt{2}\epsilon$, the equality of two sides then gives $\frac{a^2}{\sqrt{2}} = \sqrt{2} \Rightarrow a = \sqrt{2}$.

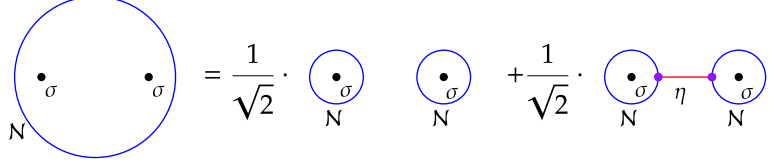


Figure 24: Performing a partial fusion on the \mathcal{N} loop circling two σ 's, where $\frac{1}{\sqrt{2}}$'s are normalizing factors.

Now we can consider the correlation function of defect operators. Take the four-point function of four $\mathcal{H}_{\mathcal{N}} \ni s_{\frac{1}{16},0}$'s attached to two \mathcal{N} 's as an example, where we denote the 12-34 channel as H and the 23-14 channel as Ξ . The four-point function has contributions from two conformal blocks, one with identity internal primary and the other with internal $\psi_{\frac{1}{2},0} \in \mathcal{H}_{\eta}$

$$\begin{aligned} \langle s(x_1)s(x_2)s(x_3)s(x_4) \rangle_H^I &= x_{13}^{-\frac{1}{8}}x_{24}^{-\frac{1}{8}} \mathcal{F}\left(\frac{1}{16}, \frac{1}{16}, \frac{1}{16}, \frac{1}{16}; 0|x\right) \\ \langle s(x_1)s(x_2)s(x_3)s(x_4) \rangle_H^\eta &= C_{ss\psi}^2 x_{13}^{-\frac{1}{8}}x_{24}^{-\frac{1}{8}} \mathcal{F}\left(\frac{1}{16}, \frac{1}{16}, \frac{1}{16}, \frac{1}{16}; \frac{1}{2}|x\right) \end{aligned} \quad (5.20)$$

where $x = \frac{x_{12}x_{34}}{x_{13}x_{24}}$. The s operators are normalized to fit $\langle s(z)s(0) \rangle = z^{-\frac{1}{8}} + \dots$. The H -junction crossing relation with the kernel being (5.17) tells us that

$$\langle s_1s_2s_3s_4 \rangle_H^I = \frac{1}{\sqrt{2}} \langle s_1s_2s_3s_4 \rangle_{\Xi}^I + \frac{1}{\sqrt{2}} \langle s_1s_2s_3s_4 \rangle_{\Xi}^\eta \quad (5.21)$$

$$\langle s_1s_2s_3s_4 \rangle_H^\eta = \frac{1}{\sqrt{2}} \langle s_1s_2s_3s_4 \rangle_{\Xi}^I - \frac{1}{\sqrt{2}} \langle s_1s_2s_3s_4 \rangle_{\Xi}^\eta \quad (5.22)$$

where $\langle s(x_1)s(x_2)s(x_3)s(x_4) \rangle$ is abbreviated to $\langle s_1s_2s_3s_4 \rangle$. On the other hand, conformal block \mathcal{F} takes the form

$$\mathcal{F}\left(\frac{1}{16}, \frac{1}{16}, \frac{1}{16}, \frac{1}{16}; 0|x\right) = (x(1-x))^{-\frac{1}{8}} \sqrt{\frac{1+\sqrt{1-x}}{2}} \quad (5.23)$$

$$\mathcal{F}\left(\frac{1}{16}, \frac{1}{16}, \frac{1}{16}, \frac{1}{16}; \frac{1}{2}|x\right) = 2(x(1-x))^{-\frac{1}{8}} \sqrt{\frac{1-\sqrt{1-x}}{2}} \quad (5.24)$$

from which we have

$$\begin{aligned} \mathcal{F}(\dots; 0|1-x) &= \frac{1}{\sqrt{2}} \mathcal{F}(\dots; 0|x) + \frac{1}{2\sqrt{2}} \mathcal{F}\left(\dots; \frac{1}{2}|x\right) \\ \mathcal{F}\left(\dots; \frac{1}{2}|1-x\right) &= \sqrt{2} \mathcal{F}(\dots; 0|x) - \frac{1}{\sqrt{2}} \mathcal{F}\left(\dots; \frac{1}{2}|x\right) \end{aligned} \quad (5.25)$$

while the relation between the two channels is exactly $x \rightarrow 1 - x$. Combining (5.20), (5.25) and (5.21) we have

$$\begin{aligned} \frac{1}{2} \left(\mathcal{F}(\dots; 0|x) - \frac{1}{2} \mathcal{F}\left(\dots; \frac{1}{2}|x\right) \right) &= C_{ss\psi}^2 \left(\mathcal{F}(\dots; 0|x) - \frac{1}{2} \mathcal{F}\left(\dots; \frac{1}{2}|x\right) \right) \\ &\Rightarrow C_{ss\psi} = \frac{1}{\sqrt{2}} \end{aligned} \quad (5.26)$$

Alternatively we can use (5.20), (5.25) and (5.22) resulting in

$$\begin{aligned} \frac{1}{2} \left(\mathcal{F}(\dots; 0|x) + \frac{1}{2} \mathcal{F}\left(\dots; \frac{1}{2}|x\right) \right) &= C_{ss\psi}^2 \left(\mathcal{F}(\dots; 0|x) + \frac{1}{2} \mathcal{F}\left(\dots; \frac{1}{2}|x\right) \right) \\ &\Rightarrow C_{ss\psi} = \frac{1}{\sqrt{2}} \end{aligned} \quad (5.27)$$

again.

Another example is the torus one-point function of ψ attached to a temporal \mathcal{N} loop via the $V_{\mathcal{N},\mathcal{N},\eta}$ junction, denoted by $\langle \psi \rangle_{T^2,\mathcal{N}}$. Such a one-point function becomes $\langle \psi \rangle_{T^2}^{\mathcal{N}}$ under S transformation, as shown in Fig.25. From the fusion rules, we know that for a pair of primaries with the same conformal weight, an $h = \frac{1}{2}$ field only receives contributions from a pair of $h = \frac{1}{16}$ primaries in the correlation function. Therefore, $\langle \psi \rangle_{T^2,\mathcal{N}}$ only receives contributions from $s_{\frac{1}{16},0}, \Lambda_{\frac{1}{16},\frac{1}{2}} \in \mathcal{H}_{\mathcal{N}}$, while $\langle \psi \rangle_{T^2}^{\mathcal{N}}$ only receives contribution from $\sigma_{\frac{1}{16},\frac{1}{16}} \in \mathcal{H}$. We can thus determine that

$$\langle \psi \rangle_{T^2,\mathcal{N}} = \frac{1}{\sqrt{2}} \eta(\tau) \left(\bar{\chi}_0(\bar{\tau}) - \bar{\chi}_{\frac{1}{2}}(\bar{\tau}) \right), \quad \langle \psi \rangle_{T^2}^{\mathcal{N}} = \eta(\tau) \bar{\chi}_{\frac{1}{16}}(\bar{\tau}) \quad (5.28)$$

where $\eta(\tau) = q^{\frac{1}{24}} \prod_{n=1}^{\infty} (1 - q^n)$ is the Dedekind η function.

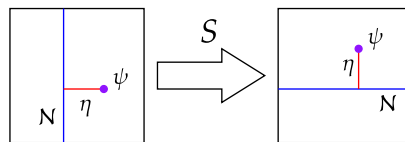


Figure 25: $\langle \psi \rangle_{T^2,\mathcal{N}}$ and $\langle \psi \rangle_{T^2}^{\mathcal{N}}$ related by an S transformation

5.4 Spin selection rule with the non-invertible \mathcal{N}

Before, we have introduced the TY category and the Ising model as a \mathbb{Z}_2 example. Below, we study the TY categories associated with the abelian finite groups Z_2 and Z_3 , and derive their spin selection rules.

5.4.1 $\text{TY}(\mathbb{Z}_2)$ spin selection rule

Remember $\text{TY}(\mathbb{Z}_n)$ has the fusion rules (5.1) and the crossing kernel (5.2), (5.4), for $n = 2$ we write again

$$F_{\mathcal{N},\mathcal{N}}^{\mathcal{N},\mathcal{N}} = \begin{pmatrix} F_{\mathcal{N},\mathcal{N}}^{\mathcal{N},\mathcal{N}}(I, I) & F_{\mathcal{N},\mathcal{N}}^{\mathcal{N},\mathcal{N}}(I, \eta) \\ F_{\mathcal{N},\mathcal{N}}^{\mathcal{N},\mathcal{N}}(\eta, I) & F_{\mathcal{N},\mathcal{N}}^{\mathcal{N},\mathcal{N}}(\eta, \eta) \end{pmatrix} = \frac{a}{\sqrt{2}} \begin{pmatrix} 1 & 1 \\ 1 & -1 \end{pmatrix}, \quad F_{\mathcal{N},\eta}^{\eta,\mathcal{N}} = -1 \quad (5.29)$$

where $a = \pm 1$.

Under a T^2 Transformation, the partition function $Z_{\mathcal{N}}$ with a temporal \mathcal{N} becomes

$$T^2 Z_{\mathcal{N}} = \text{Tr}_{\mathcal{H}_{\mathcal{N}}} \left(e^{i4\pi(L_0 - \bar{L}_0)} q^{L_0 - c/24} \bar{q}^{\bar{L}_0 - c/24} \right) \quad (5.30)$$

Alternatively, one can apply the crossing relation as shown in Fig.26, obtaining

$$T^2 Z_{\mathcal{N}} = \text{Tr}_{\mathcal{H}_{\mathcal{N}}} \left(\frac{a}{\sqrt{2}} (1 + \gamma_{\eta}) q^{L_0 - c/24} \bar{q}^{\bar{L}_0 - c/24} \right) \quad (5.31)$$

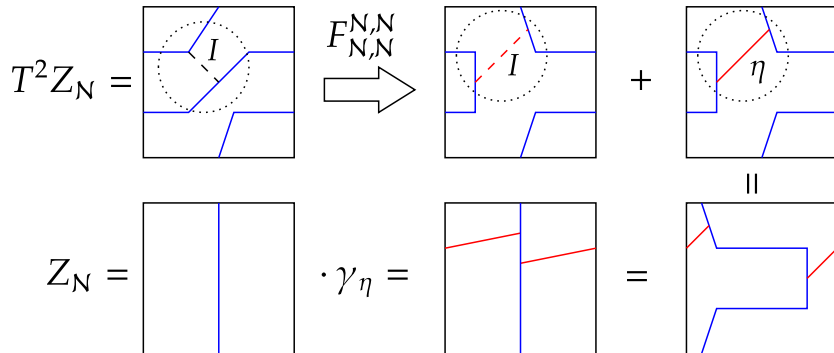


Figure 26: Applying the crossing kernel $F_{\mathcal{N},\mathcal{N}}^{\mathcal{N},\mathcal{N}}$ on $T^2 Z_{\mathcal{N}}$, where blue lines are \mathcal{N} and red lines are η . The result includes a phase γ_{η} generated by a η line.

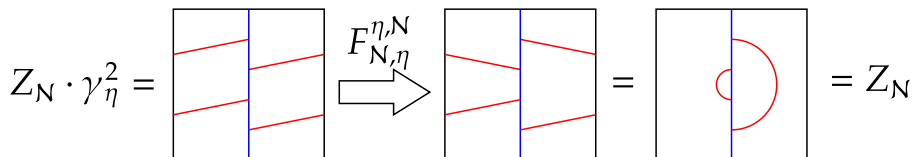


Figure 27: Illustration of $\gamma_{\eta}^2 = -1$. Note that $F_{\eta,\mathcal{N}}^{\eta,\mathcal{N}} = -1$. The η semicircle attached to the \mathcal{N} vanish by the trivial $F_{\eta,\mathcal{N}}^{\eta,\mathcal{N}}(I, \mathcal{N})$.

In order to determine γ_{η} , consider the crossing relation in Fig.27, from which we have $\gamma_{\eta} = \pm i \Rightarrow \frac{a}{\sqrt{2}} (1 + \gamma_{\eta}) = e^{\pm i \frac{2-a}{4}\pi}$. Comparing the two equations, we have the spin selection rule

$$h - \bar{h} = \frac{\mathbb{Z}}{2} + \begin{cases} \pm \frac{1}{16} & a = 1 \\ \pm \frac{3}{16} & a = -1 \end{cases} \quad (5.32)$$

We can see that the $a = 1$ case can be the critical Ising model, while the $a = -1$ case involves tensor products with other models.

5.4.2 $\text{TY}(\mathbb{Z}_3)$ spin selection rule

Our fusion rules (5.1) and the crossing kernel (5.2), (5.4) still suffice. For $n = 3$,

$$F_{\mathcal{N},\mathcal{N}}^{\mathcal{N},\mathcal{N}} = \frac{a}{\sqrt{3}} \begin{pmatrix} 1 & 1 & 1 \\ 1 & \omega & \omega^2 \\ 1 & \omega^2 & \omega \end{pmatrix}, \quad F_{\mathcal{N},\eta}^{\eta,\mathcal{N}} = F_{\mathcal{N},\eta^2}^{\eta^2,\mathcal{N}} = \omega, \quad F_{\mathcal{N},\eta}^{\eta^2,\mathcal{N}} = F_{\mathcal{N},\eta^2}^{\eta^2,\mathcal{N}} = \omega^2 \quad (5.33)$$

where $a = \pm 1$ and $\omega = e^{i\frac{2\pi}{3}}$. The derivation is similar to the $\text{TY}(\mathbb{Z}_2)$ case. Again act T^2 on $Z_{\mathcal{N}}$, this time we have

$$e^{i4\pi(h-\bar{h})} = \frac{a}{\sqrt{3}}(1 + \gamma_{\eta} + \gamma_{\eta^2}) \quad (5.34)$$

where $\gamma_{\eta}^3 = \gamma_{\eta^2}^3 = 1$. The overall angle this time becomes $\pm\frac{\pi}{6}, \pm\frac{\pi}{2}$ for $a = 1$, and $\pm\frac{5\pi}{6}, \pm\frac{\pi}{2}$ for $a = -1$. Then

$$h - \bar{h} = \frac{\mathbb{Z}}{2} + \begin{cases} \pm\frac{1}{24}, \pm\frac{1}{8} & a = 1 \\ \pm\frac{5}{24}, \pm\frac{1}{8} & a = -1 \end{cases} \quad (5.35)$$

The cases with $n > 3$ can be handled similarly.

5.5 Brief introduction to TDLs in other models

Apart from the critical Ising models, one can also find TDLs in the tricritical, the Lee-Yang model, the three-state Potts model, etc. Here we quickly go over the basic properties of TDLs in these models without getting into the details.

5.5.1 Tricritical Ising model

The $c = \frac{7}{10}$ tricritical Ising model is the minimal model $\mathcal{M}_{4,5}$ with the primaries:

$$\mathbf{1}_{0,0}, \epsilon_{\frac{1}{10}, \frac{1}{10}}, \epsilon'_{\frac{3}{5}, \frac{3}{5}}, \epsilon''_{\frac{3}{2}, \frac{3}{2}}, \sigma_{\frac{3}{80}, \frac{3}{80}}, \sigma'_{\frac{7}{16}, \frac{7}{16}} \quad (5.36)$$

and Verlinde lines $\eta, \mathcal{W} = \mathcal{L}_{\phi_{1,3}}, \mathcal{N} = \mathcal{L}_{\phi_{2,1}}, \eta\mathcal{W}, \mathcal{W}\mathcal{N}$ with actions:

$$\begin{array}{ccccccc} & 1 & \epsilon & \epsilon' & \epsilon'' & \sigma & \sigma' \\ \eta : & 1 & 1 & 1 & 1 & -1 & -1 \\ \mathcal{W} : & \zeta & -\zeta^{-1} & -\zeta^{-1} & \zeta & -\zeta^{-1} & \zeta \\ \mathcal{N} : & \sqrt{2} & -\sqrt{2} & \sqrt{2} & -\sqrt{2} & 0 & 0 \end{array} \quad (5.37)$$

where $\zeta = \frac{\sqrt{5}+1}{2}$. The fusion rules are

$$\eta^2 = I, \quad \mathcal{N}^2 = I + \eta, \quad \mathcal{W}^2 = I + \mathcal{W} \quad (5.38)$$

The spin selection rules are

$$\mathcal{H}_{\mathcal{W}} : h - \bar{h} \in \mathbb{Z} + \left\{ 0, \pm \frac{2}{5} \right\} \quad (5.39)$$

$$\mathcal{H}_{\mathcal{N}} : h - \bar{h} \in \frac{\mathbb{Z}}{2} \pm \frac{1}{16} \quad (5.40)$$

5.5.2 Lee-Yang model

The $c = -\frac{22}{5}$ tricritical Ising model is the minimal model $\mathcal{M}_{5,2}$ with only two Verlinde lines $I, \mathcal{W} = \mathcal{L}_{\phi_{1,2}}$ with actions:

$$\mathcal{W} : \begin{array}{ccc} 1 & \phi_{1,2} \\ -\zeta^{-1} & \zeta \end{array} \quad (5.41)$$

where $\zeta = \frac{\sqrt{5}+1}{2}$. The fusion rule can only be

$$\mathcal{W}^2 = I + \mathcal{W} \quad (5.42)$$

with the crossing kernel [32]

$$F_{\mathcal{W},\mathcal{W}}^{\mathcal{W},\mathcal{W}} = \begin{pmatrix} F_{\mathcal{W},\mathcal{W}}^{\mathcal{W},\mathcal{W}}(I,I) & F_{\mathcal{W},\mathcal{W}}^{\mathcal{W},\mathcal{W}}(I,\mathcal{W}) \\ F_{\mathcal{W},\mathcal{W}}^{\mathcal{W},\mathcal{W}}(\mathcal{W},I) & F_{\mathcal{W},\mathcal{W}}^{\mathcal{W},\mathcal{W}}(\mathcal{W},\mathcal{W}) \end{pmatrix} = \begin{pmatrix} -\zeta & -\zeta \\ 1 & \zeta \end{pmatrix} \quad (5.43)$$

The spin selection rule is

$$\mathcal{H}_{\mathcal{W}} : h - \bar{h} \in \mathbb{Z} + \left\{ 0, \pm \frac{2}{5} \right\} \quad (5.44)$$

5.5.3 Three-state Potts model

The $c = \frac{4}{5}$ tricritical Ising model is the minimal model $\mathcal{M}_{5,6}$ with the 12 primaries:

$$\mathbf{1}_{0,0}, \epsilon_{\frac{2}{5},\frac{2}{5}}, X_{\frac{7}{5},\frac{7}{5}}, Y_{\frac{3}{3},\frac{3}{3}}, \phi_{\frac{7}{5},\frac{2}{5}}, \tilde{\phi}_{\frac{2}{5},\frac{7}{5}}, \Omega_{3,0}, \tilde{\Omega}_{0,3}, \sigma_{\frac{1}{15},\frac{1}{15}}, \sigma_{\frac{1}{15},\frac{1}{15}}^*, Z_{\frac{2}{3},\frac{2}{3}}, Z_{\frac{2}{3},\frac{2}{3}}^* \quad (5.45)$$

This model is not diagonal, but can be regarded as one if we pick out the spin 3 operators Ω, Ω^* to form a W_3 -algebra together with $L_n, \bar{L}_n \subset T$. From this viewpoint, there are six primaries: $1, \epsilon, \sigma, \sigma^*, Z, Z^*$, with the corresponding Verlinde lines $I, \eta \in \mathbb{Z}_3, \mathbb{Z}_3 \cdot \mathcal{W}$ and the fusion rules $\mathcal{W}^2 = I + \mathcal{W}$.

With respect to the Virasoro algebra, however, one can find more TDLs including an invertible C , two non-oriented non-invertible $\mathcal{N}, \mathcal{N}' = C\mathcal{N}$, and $C \cdot \mathbb{Z}_3, C \cdot \mathbb{Z}_3 \cdot \mathcal{W}, \mathcal{W}\mathcal{N}, \mathcal{W}\mathcal{N}'$, with the fusion rules $\mathcal{N}^2 = \mathcal{N}'^2 = I + \eta + \eta^2$. Another property of this model is that its \mathbb{Z}_2 -orbifold CFT is the $c = \frac{4}{5}$ diagonal tetracritical Ising model $\mathcal{M}_{5,6}$, where there are 10 Verlinde TDLs, all of which can be derived from the TDLs above.

References

- [1] John Cardy. Boundary conformal field theory, 2008.
- [2] Masaki Oshikawa and Ian Affleck. Defect lines in the ising model and boundary states on orbifolds. *Physical Review Letters*, 77(13):2604–2607, September 1996.
- [3] Masaki Oshikawa and Ian Affleck. Boundary conformal field theory approach to the critical two-dimensional ising model with a defect line. *Nuclear Physics B*, 495(3):533–582, June 1997.
- [4] V.B. Petkova and J.-B. Zuber. Generalised twisted partition functions. *Physics Letters B*, 504(1–2):157–164, April 2001.
- [5] Jürgen Fuchs, Ingo Runkel, and Christoph Schweigert. Tft construction of rcft correlators i: partition functions. *Nuclear Physics B*, 646(3):353–497, December 2002.
- [6] Jürgen Fuchs, Ingo Runkel, and Christoph Schweigert. Tft construction of rcft correlators ii: unoriented world sheets. *Nuclear Physics B*, 678(3):511–637, February 2004.
- [7] Jürgen Fuchs, Ingo Runkel, and Christoph Schweigert. Tft construction of rcft correlators. *Nuclear Physics B*, 694(3):277–353, August 2004.
- [8] Jürgen Fuchs, Ingo Runkel, and Christoph Schweigert. Tft construction of rcft correlators iv:. *Nuclear Physics B*, 715(3):539–638, May 2005.
- [9] Jürg Fröhlich, Jürgen Fuchs, Ingo Runkel, and Christoph Schweigert. Kramers-wannier duality from conformal defects. *Physical Review Letters*, 93(7), August 2004.
- [10] Jürg Fröhlich, Jürgen Fuchs, Ingo Runkel, and Christoph Schweigert. Duality and defects in rational conformal field theory. *Nuclear Physics B*, 763(3):354–430, February 2007.
- [11] Thomas Quella, Ingo Runkel, and Gérard M.T Watts. Reflection and transmission for conformal defects. *Journal of High Energy Physics*, 2007(04):095–095, April 2007.
- [12] Jürgen Fuchs, Ingo Runkel, and Christoph Schweigert. The fusion algebra of bimodule categories. *Applied Categorical Structures*, 16(1–2):123–140, July 2007.
- [13] Jürgen Fuchs, Matthias R Gaberdiel, Ingo Runkel, and Christoph Schweigert. Topological defects for the free boson cft. *Journal of Physics A: Mathematical and Theoretical*, 40(37):11403–11440, August 2007.

- [14] C Bachas and I Brunner. Fusion of conformal interfaces. *Journal of High Energy Physics*, 2008(02):085–085, February 2008.
- [15] Liang Kong and Ingo Runkel. Cardy algebras and sewing constraints, i. *Communications in Mathematical Physics*, 292(3), August 2009.
- [16] V. B. Petkova. On the crossing relation in the presence of defects. *Journal of High Energy Physics*, 2010(4), April 2010.
- [17] Alexei Kitaev and Liang Kong. Models for gapped boundaries and domain walls. *Communications in Mathematical Physics*, 313(2):351–373, June 2012.
- [18] Nils Carqueville and Ingo Runkel. Orbifold completion of defect bicategories. *Quantum Topology*, 7(2):203–279, February 2016.
- [19] Ilka Brunner, Nils Carqueville, and Daniel Plencner. A quick guide to defect orbifolds, 2013.
- [20] Liang Kong, Qin Li, and Ingo Runkel. Cardy algebras and sewing constraints, ii. *Advances in Mathematics*, 262:604–681, September 2014.
- [21] Marcel Bischoff, Yasuyuki Kawahigashi, Roberto Longo, and Karl-Henning Rehren. *Tensor Categories and Endomorphisms of von Neumann Algebras: with Applications to Quantum Field Theory*. Springer International Publishing, 2015.
- [22] Lakshya Bhardwaj and Yuji Tachikawa. On finite symmetries and their gauging in two dimensions. *Journal of High Energy Physics*, 2018(3), March 2018.
- [23] Chi-Ming Chang, Ying-Hsuan Lin, Shu-Heng Shao, Yifan Wang, and Xi Yin. Topological defect lines and renormalization group flows in two dimensions. *Journal of High Energy Physics*, 2019(1), January 2019.
- [24] Chi-Ming Chang, Jin Chen, and Fengjun Xu. Topological defect lines in two dimensional fermionic cfts. *SciPost Physics*, 15(5), November 2023.
- [25] Philippe Di Francesco, Pierre Mathieu, and David Sénéchal. *Conformal field theory*. Graduate texts in contemporary physics. Springer, New York, NY, 1997.
- [26] Chi-Ming Chang and Ying-Hsuan Lin. On exotic consistent anomalies in $(1+1)d$: A ghost story. *SciPost Physics*, 10(5), May 2021.
- [27] Robbert Dijkgraaf and Edward Witten. Topological gauge theories and group cohomology. *Communications in Mathematical Physics*, 129:393–429, 1990.
- [28] Cumrun Vafa. Modular invariance and discrete torsion on orbifolds. *Nuclear Physics B*, 273(3):592–606, 1986.

- [29] Ilka Brunner, Nils Carqueville, and Daniel Plencner. Discrete torsion defects. *Communications in Mathematical Physics*, 337(1):429–453, February 2015.
- [30] H. A. Kramers and G. H. Wannier. Statistics of the two-dimensional ferromagnet. part ii. *Phys. Rev.*, 60:263–276, Aug 1941.
- [31] Daisuke Tambara and Shigeru Yamagami. Tensor categories with fusion rules of self-duality for finite abelian groups. *Journal of Algebra*, 209(2):692–707, 1998.
- [32] Gregory W. Moore and Nathan Seiberg. Classical and Quantum Conformal Field Theory. *Commun. Math. Phys.*, 123:177, 1989.

中文摘要

在一般的量子场论中，时空对称性是洛伦兹（Lorentz）不变性。而共形场论（CFT）则将洛伦兹不变提升到共形不变。洛伦兹不变要求变换前后的距离度量保持不变，而共形不变则允许距离度量乘以一个因子，从而其在洛伦兹不变原有的平移、旋转不变的基础上增加了放缩（dilation）、特殊共形变换（Special Conformal Transformation, SCT）不变。其中特殊共形变换相当于依次进行反转 ($x \rightarrow \frac{x}{x^2}$)、平移、反转变换，是一种囊括了反转变换的同时又具有无穷小版本的构造。对称性的提高共形场论具有更加丰富的结构。进一步地，二维欧氏时空下的共形变换等价于全纯函数映射，从而具有无穷维的无穷小变换生成元，使得二维共形场论更为特别、容纳了许多具体模型的解析解。此外二维共性变换中全局可逆的部分也正是平移、旋转、放缩、SCT 变换的二维版本，它们生成了莫比乌斯群 $SL(2, \mathbb{C})$ 。

二维共形场论还具有的特征是由径向量子化得到的态-算符对应，以及由能动张量的洛朗展开与 Ward-Takahashi 恒等式得到的算符乘积展开（OPE）、初级与后裔场（primaries and descendants）、Virasoro 代数等。一个具体的二维共形场论模型通常由初级场和它们的算符乘积展开刻画，对应于一般的量子场论中的关联函数。

在共形场论的语境下，已经有许多关于“缺陷”这一对象的研究，包括边界条件、线缺陷/界面等，这些对象可以通过它们对于局域算符（local operators）的作用来定义。一个简单的例子是一个全局对称群（Global symmetry group） G 中的某个变换 g ，它应当是一个保持算符乘积展开不变的作用在局域算符的线性变换。而它对局域算符的作用可以被视为一个环绕着该局域算符的拓扑线缺陷（Topological defect line, TDL）的收缩。这样的对应于某个全局对称变换的拓扑线缺陷在本文中被称为可逆的（invertible），因为它作为一个群元必然有其逆元。

这些对应于全局对称性的可逆拓扑线缺陷应当具有局域性，这意味着它们可以以缺陷算符（defect operators）为终点，而这些缺陷算符则扩展了原本仅考虑局域算符的算符乘积展开。在全局对称性连续的情况下，诺特定理保证了一个守恒流的存在，而可逆拓扑线缺陷可以由这一守恒流的围道积分定义。在全局对称性离散的情况下，可逆拓扑线缺陷可以被视为诺特定理的离散版本。它对于对称性在局域算符上的作用有着并不平凡的影响。

除此之外，同样存在着并不对应于任何全局对称性的拓扑线缺陷，并且这在二维共形场论中非常常见。这些更一般的拓扑线缺陷遵循融合代数规则（fusion rule），而并不构成群结构。同时在拆分-重连这些拓扑线缺陷时，还需要遵守非平凡的交错关系（crossing relation），在融合范畴（fusion category）的数学语言下也就是五边形恒等式。

在对角的有理共形场论中，存在着一类被称为 Verlinde 线的拓扑线缺陷。这些 Verlinde 线的融合代数规则在形式上与该有理共形场论的手性顶点代数的表示所遵循的规则相同，然而对于 Verlinde 线的物理理解则并不同于算符乘积展开。

本文的结构如下：首先，我们将回顾共形场论的基础理论和会在本文中有所运用的重要概念，包括环面配分函数与环面模群、极小模型、共形块、有理共形场论等。而后，我们将从一系列以物理意义作为动机的定义和性质开始介绍拓扑线缺陷。我们将介绍拓扑线缺陷如何作用在局域算符、缺陷算符上，如何对其进行具体的融合操作，如何定义带有拓扑线缺陷的关联函数，如何定义其共轭，以及拓扑线缺陷的局域性质和其在环面上的模协变性（modular covariance）。而基于这些性质，我们将推导 H 型汇合点的交错关系与五边形恒等式，关于拓扑线缺陷的真空期望和缺陷希尔伯特空间的条件，以及拓扑线缺陷的融合代数规则的系数。同时我们还会介绍拓扑线缺陷可能出现的同痕异常（isotopy anomaly），这可能使得拓扑线缺陷的真空期望与其在空的平面上环绕一圈的结果相差一个相位因子。

接下来，我们将着重于可逆拓扑线缺陷，介绍其与't Hooft 异常、轨形（orbifold）等概念之间的关系。通过将't Hooft 异常带来的交错关系中的相位因子代入五边形恒等式，再结合一个物理上等价的相位变换，我们可以得到 $H^3(G, U(1))$ 这一能够分类't Hooft 异常的群上同调，并能进一步得到 $H^2(G, U(1))$ 这一能够分类轨形的群上同调。我们还会从异常出发，推导一个关于可逆线缺陷的缺陷希尔伯特空间的自旋规则。我们会以紧致化在 S^1 上的自由玻色子的 $U(1)$ 变换作为具体例子来说明这一规则。

随后，我们将关注有理共形场论中的一般的拓扑线缺陷，包括不可逆拓扑线缺陷。我们会先介绍一类特殊的不可逆拓扑线缺陷 \mathcal{N} ，它能够和循环群 \mathbb{Z}_n 组合、得到一组良好的融合代数规则，也就是 Tambara-Yamagami 融合范畴。线缺陷 \mathcal{N} 实际上描述了一个具有循环群 \mathbb{Z}_n 对称性的二维共形场论与其在轨形上的版本的对偶关系。线缺陷 \mathcal{N} 的一个例子是在伊辛模型中，伊辛模型的循环对称群就是 \mathbb{Z}_2 ，而 \mathcal{N} 则可被看作一种对于有序-无序对偶的推广。

而后我们会介绍有理共形场论中 Verlinde 线的概念，并具体地在伊辛模型中得到交错关系，由此推导线缺陷对于缺陷算符的作用、缺陷算符的算符乘积展开系数、缺陷希尔伯特空间的环面配分函数等。接着，我们将基于 \mathcal{N} 和循环群 \mathbb{Z}_n 的融合代数规则推导出 \mathcal{N} 的缺陷希尔伯特空间的自旋规则，包括 $n = 2$ 和 $n = 3$ 的情况。最后，我们会简要介绍一些其它有理共形场论模型中的拓扑线缺陷，包括三临界伊辛模型、李-杨模型、三态 Potts 模型。